DEVELOPMENT OF HYPOXIA INDUCIBLE FACTOR-1 ALPHA AND GHRELIN-LOADED CORE/SHELL FIBROUS SCAFFOLDS FOR IMPROVING VASCULARIZATION AND OSTEOGENESIS

A THESIS SUBMITTED TO
THE GRADUATE SCHOOL OF NATURAL AND APPLIED SCIENCES
OF
MIDDLE EAST TECHNICAL UNIVERSITY

BY

EREN KÜÇÜK

IN PARTIAL FULFILLMENT OF THE REQUIREMENTS
FOR
THE DEGREE OF MASTER OF SCIENCE
IN
BIOMEDICAL ENGINEERING

DECEMBER 2023

Approval of the thesis:

DEVELOPMENT OF HYPOXIA INDUCIBLE FACTOR-1 ALPHA AND GHRELIN LOADED CORE/SHELL FIBROUS SCAFFOLDS FOR IMPROVING VASCULARIZATION AND OSTEOGENESIS

submitted by **EREN KÜÇÜK** in partial fulfillment of the requirements for the degree of **Master of Science** in **Biomedical Engineering, Middle East Technical University** by,

Prof. Dr. Halil Kalıpçılar
Dean, Graduate School of **Natural and Applied Sciences**

Prof. Dr. Vilda Purutçuoğlu
Head of the Department, **Biomedical Engineering**

Prof. Dr. Dilek Keskin
Supervisor, **Biomedical Engineering, METU**

Prof. Dr. Ayşen Tezcaner
Co-Supervisor, **Biomedical Engineering, METU**

Examining Committee Members:

Prof. Dr. Sreeparna Banerjee
Biological Sciences, METU

Prof. Dr. Dilek Keskin
Engineering Sciences, METU

Prof. Dr. Ayşen Tezcaner
Engineering Sciences, METU

Prof. Dr. Pelin Mutlu
Biotechnology Institute, Ankara University

Assist. Prof. Dr. Özge Erdemli
Molecular Biology and Genetics, Başkent University

Date: 11.12.2023

I hereby declare that all information in this document has been obtained and presented by academic rules and ethical conduct. I also declare that, as required by these rules and conduct, I have fully cited and referenced all material and results that are not original to this work.

Name Last name: Eren Küçük

Signature:

ABSTRACT

DEVELOPMENT OF HYPOXIA-INDUCIBLE FACTOR-1 ALPHA AND GHRELIN-LOADED CORE/SHELL FIBROUS SCAFFOLDS FOR IMPROVING VASCULARIZATION AND OSTEOGENESIS

Küçük, Eren
Master of Science, Biomedical Engineering
Supervisor: Prof. Dr. Dilek Keskin
Co-Supervisor: Prof. Dr. Ayşen Tezcaner

December 2023, 89 pages

The purpose of bone tissue engineering is to develop biocompatible materials, that have adjustable durability depending on the area to be applied, and promote cell adhesion and growth to improve the bone regeneration process. There are still some restrictions and risks in the clinical treatments used today. In this thesis, the focus is on increasing vascularization, one of the limitations of bone tissue engineering, by using a special protein and enhancing regeneration using a bone regenerative peptide. The basic approach is stimulating the necessary pathways by local controlled release of two proteins: Hypoxia Inducing Factor-1 α; HIF1α (a transcription factor) and ghrelin(a peptide hormone) to support vascularization and bone regeneration, respectively. To investigate the potential of these biological molecules in a local delivery system a new scaffold was developed with cellulose acetate (CA), polycaprolactone (PCL), and gelatin (GEL) polymers. Scaffolds of double-layered fibers (core/shell fibers) were formed with CA in the shell and PCL-Gel in the core using the coaxial wet electrospinning method.

The shell layer of the scaffold was loaded with HIF1-α protein to provide early release of this protein from the scaffold to start angiogenesis earlier when applied in vivo. To support bone regeneration throughout the healing period Ghrelin was loaded to the inner (core) layer of the fibers (PCL-GEL) of the scaffold for more sustained and controlled release. Initial structural characterizations by SEM analysis and observations on the final solid form were used to select the best scaffold composition and production parameters. Upon optimization studies, the best composition for fibrous scaffold production was found as CA (12 %) and PCL: Gel (80:20 ratio) with 10 % total polymer concentration which presented homogenous fiber diameters and durable 3D form. For 14 days of degredation, the dry weight of the scaffold did not change. As a result of 14-day swelling analysis, 1200% swelling was observed. Release experiments with a single protein/peptide loaded to different layers of the fibers of scaffolds provided the fast release of HIF1 α (within 2 days) from scaffolds and slower release of Ghrelin (extending up to 10 days) as initially aimed.

In vitro experiments with scaffolds were performed both with an endothelial cell line (HUVEC) and a bone osteoblast cell line (HFOB). In vitro, scaffold cell culture studies with HUVEC cells showed that HIF1-ɑ increases VEGF production. In vitro, scaffold cell culture studies with HFOB cells showed that ghrelin hormone increases cell viability. The effect on osteogenic differentiation investigated by Alkaline phosphatase enzyme (ALP) activity analysis showed no significant effect of ghrelin on the 7th-day results, but the ALP activity results of the cells exposed to ghrelin were approximately 2.5 times higher than the control group on the 14th day.

The developed dual protein/peptide delivery system is found to have the potential for bone tissue regeneration and can be suggested for further in vivo studies.

Keywords: Bone tissue engineering, Angiogenesis in bone tissue, Coaxial electrospinning, Hypoxia-inducible factor 1-alpha, Ghrelin.

ÖZ

VASKÜLARİZASYON VE OSTEOGENEZİN İYİLEŞTİRİLMESİ İÇİN HİPOKSİ İLE İNDÜKLENEBİLİR FAKTÖR-1 ALFA VE GHRELİN YÜKLÜ ÇEKİRDEK/KABUK FİBRÖZ DOKU İSKELELERİNİN GELİŞTİRİLMESİ

Küçük, Eren
Yüksek Lisans, Biyomedikal Mühendisliği
Tez Yöneticisi: Prof. Dr. Dilek Keskin
Ortak Tez Yöneticisi: Prof. Dr. Ayşen Tezcaner

Aralık 2023, 89 sayfa

Kemik doku mühendisliğinin amacı, biyouyumlu, uygulanacak bölgeye göre ayarlanabilir dayanıklılığa sahip ve hücre yapışmasını ve büyümesini teşvik eden malzemeler geliştirerek kemik rejenerasyon sürecini iyileştirmektir. Günümüzde kullanılan klinik tedavilerde hala bazı kısıtlamalar ve riskler bulunmaktadır. Bu tez çalışması, kemik doku mühendisliğinin sınırlamalarından biri olan yetersiz vaskülarizasyon üzerine odaklanmaktadır ve lokal uygulama için güvenli bir kemik rejeneratif peptid kullanımı konusunu ele almaktadır. Temel yaklaşım, iki proteinin, Hipoksi İndükleyen Faktör-1α (HIF1α; bir transkripsiyon faktörü) ve ghrelinin (bir peptid hormonu) lokal kontrollü salınımı ile gerekli yolakları uyararak kemik rejenerasyonunu ve vaskülarizasyonu desteklemektir. Bu proteinlerin lokal uygulama sistemindeki potansiyelini araştırmak için selüloz asetat (CA), polikaprolakton (PCL) ve jelatin (GEL) polimerlerinden oluşan yeni bir iskele geliştirilmiştir. Koaksiyel ıslak elektro-eğirme yöntemi kullanılarak dış katmanda CA ve iç katmanda PCL-Jelatin içeren çift katmanlı lifler (çekirdek/kabuk lifler) oluşturulmuştur.

İskelelerin kabuk tabakası, in vivo uygulandığında anjiyogenez sürecini daha erken başlatmak için HIF1-α proteini ile yüklenmiştir. Ghrelin ile kontrollü salınımı destekleyen bir kemik doku mühendisliği iskele geliştirmek için, iç (çekirdek) katmana PCL-Jelatin polimer karışımı yüklenmiştir. SEM analizi ve nihai katı form üzerinde yapılan gözlemler, en iyi iskele bileşimini ve üretim parametrelerini seçmek için kullanılmıştır. Optimizasyon çalışmaları sonucunda, lifli iskele üretimi için en iyi bileşim, homojen lif çapları ve dayanıklı 3 boyutlu form sunan CA (%12) ve PCL:Jelatin 80:20 oranında %10 toplam polimer konsantrasyonu olarak belirlenmiştir. İskelelerin bozunma ve şişme analizi, iskelelerde kuru ağırlıkta 14 günlük bozunma deneylerinde ağırlık değişimi gözlemlenmemiştir. Şişmenin %1200 olduğunu görülmüştür. In vitro salınım deneyleri, iskelelerden hızlı bir HIF1α salınımı (2 gün içinde) ve amaçlandığı gibi daha yavaş bir ghrelin salınımı (10 güne kadar uzayan) sağlamıştır.

İskelelerle yapılan in vitro deneyler hem endotel hücre hattı (HUVEC) hem de kemik osteoblast hücre hattı (HFOB) ile gerçekleştirilmiştir. HUVEC hücreleriyle yapılan in vitro iskele hücre kültürü çalışmaları, HIF1-ɑ'nın VEGF üretimini arttırdığını göstermiştir. HFOB hücreleriyle yapılan in vitro iskele hücre kültürü çalışmaları, ghrelin hormonunun hücre canlılığını arttırdığını göstermiştir. Osteoblastik farklılaşma üzerindeki etki, 7. ve 14. günlerde ALP analizi ile araştırılmıştır. Ghrelin'in osteoblastik farklılaşma üzerinde 7. gün sonuçlarında önemli bir etkisi gözlenmese de, 14. gün ghrelin uygulanan hücrelerin osteoblastik farklılaşma sonuçları kontrol grubundan yaklaşık 2,5 kat daha yüksek olmuştur.

Geliştirilen çift protein/peptid salınım sisteminin kemik doku rejenerasyonu için potansiyele sahip olduğu ve ileri in vivo çalışmalar için önerilebileceği bulunmuştur.

Anahtar Kelimeler: Kemik doku mühendisliği, Kemik dokuda damarlaşma, Eş-eksenli elektro-eğirme, Hipoksi ile indüklenebilir faktör 1-alfa, Ghrelin.

To my dear family and my friends

ACKNOWLEDGMENTS

First of all, I would like to express my endless gratitude to my advisor, Prof. Dr. Dilek Keskin, for giving me the opportunity to study MSc at my dream university, for sharing her valuable knowledge throughout my master's studies, for always being by my side, and for supporting me patiently and confidently throughout my thesis process.

I would also like to thank my co-advisor, Prof. Dr. Ayşen Tezcaner, for her valuable feedback and experience, and especially for her guidance during the thesis period.

I would like to thank BIOMATEN.

I am especially grateful to Dr. Ahmet Engin Pazarçeviren, who taught me everything he knows and was always by my side, both emotionally and academically, throughout my thesis process.

I would like to thank my laboratory friends Sema Akbaba, Büşranur Yeşilyurt, and Melike Urhal for their support and enjoyable times. I would also like to thank my close friends and supporters Merve Varışlı, Gaye Munzur, Selin Kirdiş Gemici, Sena Gülener, Dr. Ekin Varlı, and Suzan Akkad with all my heart.

Finally, I would like to express my endless gratitude to my mother Feriştah Küçük and father Ali İhsan Küçük, who have always believed in me and been by my side, giving me strength; my brother Erdi Küçük and his wife Betül Küçük; my nephew Aybars Kutay Küçük, who is a source of joy for me; my dear aunts Selda Aktaş, Neşe Bilir, Derya Gelmez, and Hatice Bilgili. I would also like to thank my dear best friend Fatih Özyürek, who has always been there for me, especially in my difficult times. I am grateful to the Özhan Umur Şengül and Merve Bağcı Şengül family for all their support and help.

This thesis was financially supported by the TUBITAK 1002 project (122R120).

TABLE OF CONTENTS

LIST OF TABLES

TABLES

LIST OF FIGURES

FIGURES

LIST OF ABBREVIATIONS

ABBREVIATIONS

AA: Acetic Acid

ALP: Alkaline Phosphatase

BCA: Bicinchoninic Acid Solution

BMPs: Bone Morphogenetic Proteins

BTE: Bone Tissue Engineering

CA: Cellulose Acetate

DCM: Dichloromethane

dH_2O: Distilled Water

DMac: Dimethylacetamide

DMEM: Dulbecco's Modified Eagle Medium

DMF: Dimethylformamide

DMSO: Dimethyl sulfoxide

ELISA: Enzyme-Linked Immuno Sorbent Assay

FA: Formic Acid

FBS: Fetal Bovine Serum

GEL: Gelatine

HFIP: Hexafluro-2-propanol

HFOB: Human fetal osteoblast

HIF1 α: Human Hypoxia-inducible Factor 1 Alpha

HUVEC: Human Umbilical Cord Vein Endothelial Cells

Mw: Molecular Weight

PBS: Phosphate Buffer Saline

PCL: Polycaprolactone

SEM: Scanning Electron Microscope

VEGF: Vascular Endothelial Growth Factor

CHAPTER 1

INTRODUCTION

1.1 Bone Structure and Function

Bone is a complex tissue composed of inorganic and organic components that work together to provide strength, flexibility, and support to the body. The osseous matrix, also known as the extracellular matrix of bone tissue, comprises the intercellular substance of the bone tissue, encompassing both organic and inorganic constituents. It represents the bulk of bone mass, playing a crucial role in bone's structural integrity and functionality. The organic component of the osseous matrix predominantly consists of collagen fibers and a ground substance, while the inorganic component is composed primarily of hydroxyapatite, a mineral salt, along with other minerals (Lin et al., 2020). It is shown in more detail in Table 1.1.

Table 1.1 Bone matrix components and their function

Organic components	Collagen	Fibrillar type (Type I Type III Type V)	Fibrillar collagens are responsible for imparting tensile strength, flexibility, and a scaffold for mineral deposition during bone formation, remodeling, and repair (Lin et al., 2020).
		Non-fibrillar type (Type IV Type XIII)	Nonfibrillar collagens occur in relatively smaller amounts but are nevertheless essential

			for maintaining the integrity and function of bone tissue. Type IV collagen, a major component of basement membranes, forms the bone lining cells covering bone surfaces, while Type XIII collagen is involved in cell adhesion and signaling processes (Lin et al., 2020).
	The ground substance	Nonfibrillar amorphous material	Filling the space between collagen fibers and hydroxyapatite crystals within the bone matrix. Composed of glycoproteins, proteoglycans, and glycosaminoglycans, the ground substance contributes to the structural integrity of bone tissue (Lin et al., 2020).
	Other organic components	Osteocalcin Osteopontin Bone Sialoprotein Matrix Gla Protein Proteoglycans Glycoproteins Growth Factors (transforming growth factor-	Involves cell adhesion, signaling, bone mineralization, and calcium ion binding, regulating the interaction between cells and the bone matrix during bone remodeling or renewal, inhibiting the calcification of soft tissues, maintaining the extracellular matrix structure, regulating bone cell activities,

		beta (TGF-β), fibroblast growth factors (FGFs), and bone morphogenetic proteins (BMPs))	including proliferation, differentiation, migration, and new bone formation (Lin et al., 2020).
Inorganic components	Hydroxyapatite		Existing in crystalline form and represents the predominant component of the bone matrix, accounting for a significantly greater proportion than other matrix constituents, including Type I collagen, which contributes approximately 35% to the bone's dry weight (Lin et al., 2020).
	Other minerals	Calcium (Ca^{2+}) Phosphate (PO_4^{3-}) Magnesium (Mg^{2+}) Sodium (Na^{+}) Potassium (K^{+})	Playing a critical role in bone mineralization, contributing to the regulation of calcium levels, maintaining the body's electrolyte balance, playing a vital role in overall homeostasis, maintaining the acid-base balance in the bone, and ensuring proper bone function (Lin et al., 2020).

1.2 Bone Regeneration

The healing process of bone injuries occurs in three stages: inflammation, repair, and remodeling (Figure 1.). There is a lot of overlap between these phases, though. Mesenchymal stem cells are essential to the healing process, which is facilitated by principal cells and their secretions. The periosteum and endosteum are the two main sources from which they are delivered. Inflammatory cells, endothelial cells, fibroblasts, osteoblasts, and osteoclasts are among the other entities implicated (Bahney et al., 2019; Marsell & Einhorn, 2011).

The first stage, lasting one to five days, begins immediately after the injury. The blood vessels that feed the bone are torn, causing a hematoma to form at the site of the injury. This hematoma provides a temporary environment for healing (Marsell & Einhorn, 2011). The injury also causes the release of tumor necrosis factor-alpha (TNF-α), bone morphogenetic proteins, and interleukins. These proteins attract macrophages, monocytes, and lymphocytes to the area. While the damage is being cleared by these molecules, vascular endothelial growth factor (VEGF) is released, which is essential for the initiation of the healing process (Sheen et al., 2023).

The second stage, lasting from the 5th to the 28th day of healing, is the repair phase. VEGF release initiates angiogenesis, the process of forming new blood vessels that are necessary to nourish the area (Glowacki, 1998; Hausman et al., 2001). This allows the tissue within the hematoma to begin to develop. More mesenchymal stem cells are recruited to the area and begin to differentiate. As a result of this stage, chondrogenesis begins and a collagen-rich fibrocartilage network covered with hyaline cartilage forms at the ends of the injury. This cartilaginous structure begins to ossify. RANK-L is released, which stimulates the further differentiation of osteoclasts and osteoblasts. The cartilaginous callus begins to mineralize. New blood vessel formation allows for the arrival of more stem cells in the area. At the end of the repair stage, a hard, calcified callus made of immature bone is formed (L. Claes et al., 1997; L. E. Claes et al., 1998).

The remodeling phase, which begins on the 18th day of the repair phase and then varies in duration depending on the individual, begins to remodel the hard callus. This process involves resorption by osteoclasts and new bone formation by osteoblasts. The central part of the callus is replaced by compact bone, while the edges of the callus are replaced by lamellar bone. Vascular remodeling also redevelops in this process (Sheen et al., 2023).

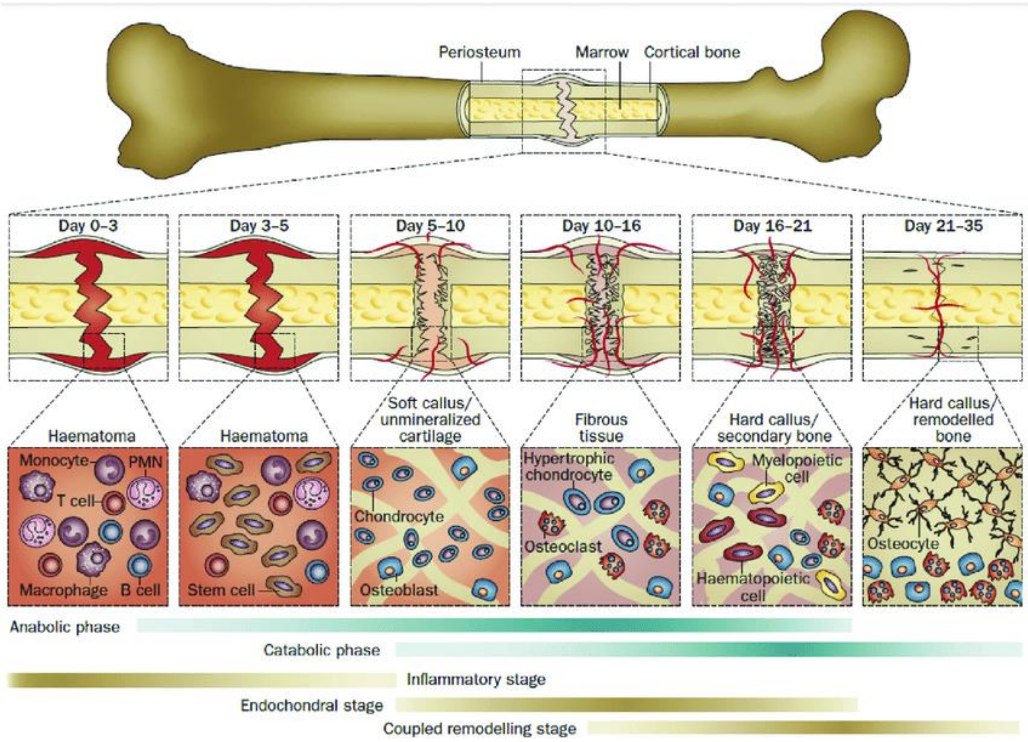

Figure 1. Diagram showing the many stages of cellular activity, biological processes, and the normal healing process for fractures (Wang & Yeung, 2017).

1.3 Bone Defects and Diseases Requiring Biomaterial Use

Bone defects are structural losses in the bone that can arise from various causes such as injuries, surgical procedures, infections, or underlying medical conditions (Figure 2.) These defects can lead to discomfort, impaired stability, and compromised functionality, and may not readily heal on their own (Zhou et al., 2021).

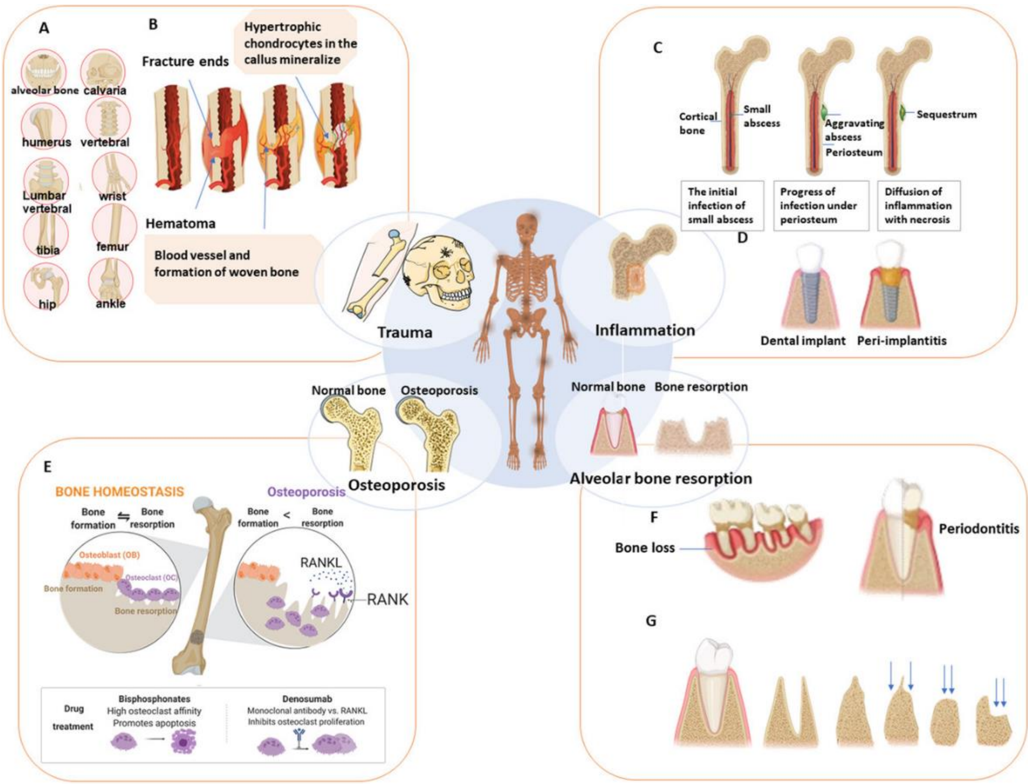

Figure 2. Primary reasons for bone loss. (Zhou et al., 2021).

1.4 Bone Tissue Engineering

Bone tissue engineering (BTE) is a research field that aims to develop new implantable biocompatible materials to overcome the limitations of clinical applications for the treatment of challenging segmental and limited skeletal defects (Dixon & Gomillion, 2021). Three key areas of study in bone tissue engineering are matrix, stem cells, and growth factors, often known as bioactive substances (drugs, proteins) (Figure 3) (Kneser et al., 2002). The ECM (3D scaffold) plays a crucial role in tissue engineering by providing mechanical support, cell attachment sites, and signaling molecules (Kneser et al., 2002). Growth factors play a critical role in bone formation by stimulating osteogenic cell proliferation and differentiation, and two important factors include bone morphogenetic proteins (BMPs) and basic fibroblast growth factor (bFGF), which can be incorporated into tissue engineering constructs for sustained release and improved efficacy (Kneser et al., 2002).

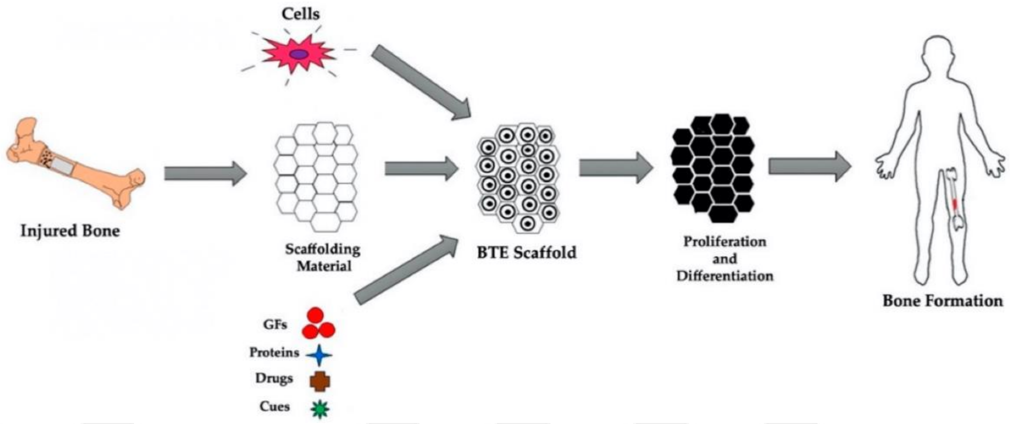

Figure 3. Three main components of BTE (Dixon & Gomillion, 2021).

1.4.1 Biomaterials Used in Bone Tissue Engineering

Biomaterials are engineered materials designed to interact with living organisms predictably and beneficially. They can repair bone defects by providing a framework for new bone growth, delivering therapeutic agents to promote bone healing, and preventing infections (Lalwani et al., 2016). Many different biomaterials as natural polymers, synthetic polymers, bioceramics, and composite biometarials can be used to repair bone defects. Each biomaterial has its advantages and disadvantages (Lalwani et al., 2016; Yang et al., 2023; Yue et al., 2020).

1.4.1.1 Synthetic Polymers

Synthetic polymers offer excellent control over their properties, making them attractive for bone tissue engineering (Shi et al., 2016). Aliphatic polyesters like PLA, PGA, and PLGA are widely used due to their biodegradability and tunable degradation rates. However, surface modifications are often needed to improve cell recognition and osteoconductivity (D. X. Wang et al., 2013). PCL, with higher crystallinity and hydrophobicity, also requires surface modifications or copolymerization to enhance its performance (Baker et al., 2012a). PVA, with its water solubility and crystallinity dependent on the degree of hydroxylation, finds applications in bone regeneration (Baker et al., 2012b). PPE, with potential osteoinductive capacity, can be used to modify other polymers and promote bone formation (Benoit et al., 2008). PTMC, an amorphous biocompatible polymer, shows promising results in guided bone regeneration (Van Leeuwen et al., 2012). Biodegradable PUs, with tunable properties and high mechanical strength, are gaining attention in bone tissue engineering, often combined with inorganic materials and bioactive substances (Huang et al., 2009). Polypeptides like γ-PGA and polylysine contribute to bone regeneration through their specific properties and are often used in combination with other materials (Hsieh et al., 2005). Overall, synthetic polymers offer a versatile and promising toolkit for designing and engineering bone tissue.

1.4.1.1.1 Polycaprolactone (PCL)

PCL is a biodegradable polyester (Figure 4.). It is a semi-crystalline aliphatic polymer with a glass transition temperature of -60°C and a melting temperature that ranges from 59 to 64°C, or above body temperature. As a result, the semi-crystalline PCL reaches a rubbery state at physiological temperature, giving it exceptional mechanical properties (high strength, elasticity depending on its molecular weight) and high toughness (Bezwada et al., 1995). Due to its non-toxicity and tissue compatibility, it is frequently utilized in drug delivery applications, resorbable sutures, and scaffolds for regenerative medicine. Under physiological conditions, PCL is broken down by microorganisms or by the hydrolysis of its aliphatic ester linkage, with a longer degradation time of two to three years. PCL degrades the slowest among these materials because its repeating units contain five hydrophobic –CH_2 moieties (Engelberg & Kohn, 1991).

PCL-based composites are promising materials for bone tissue engineering. PCL itself has several beneficial properties, including biocompatibility, low cost, and a slow degradation rate. However, its hydrophobicity, low bioactivity, and slow degradation rate can limit its applications. Combining PCL with other materials can address these limitations and improve its properties for bone regeneration (Gharibshahian et al., 2023).

- PCL/ceramic composites: Ceramics like hydroxyapatite and β-tricalcium phosphate can improve the mechanical properties, bioactivity, hydrophilicity, and biodegradability of the composite (Gharibshahian et al., 2023).
- PCL/polymer composites: Polymers like PLA, PLGA, and gelatin can improve the mechanical properties, biocompatibility, and degradation rate of the composite. Decellularized tissues can also be combined with PCL to promote bone regeneration, cell adhesion, and osteoblast proliferation (Gharibshahian et al., 2023).
- PCL/metal composites: Metals like magnesium and zinc can improve the mechanical properties, bioactivity, degradation rate, and osteogenesis of the composite (Gharibshahian et al., 2023).

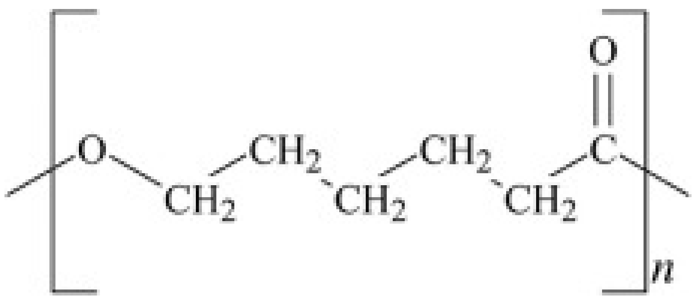

Figure 4. Chemical structure of PCL (McKeen, 2021).

1.4.1.2 Natural and Natural Origin Polymers

Naturally derived polymers such as collagen, gelatin, silk fibroin, and chitosan hold significant promise for bone tissue engineering due to their similarity to the extracellular matrix and their ability to support cell adhesion and function (Pina et al., 2015). Collagen, the major protein component of bone tissue, can be processed into various forms including hydrogels, sponges, and fibrous scaffolds (L. Wang & Stegemann, 2010). Gelatin, its denatured form, offers high water solubility and lower cost (Visser et al., 2015). Silk fibroin possesses remarkable mechanical properties and its degradation rate can be easily controlled (Liu et al., 2015). Chitosan, a positively charged polysaccharide, can electrostatically interact with negatively charged molecules and membranes (Dhivya et al., 2015). These polymers are often combined with inorganic materials like calcium phosphates (CaPs) to enhance mechanical strength and osteoconductivity. Studies have shown that these composite scaffolds promote cell proliferation, differentiation, and bone regeneration, demonstrating their potential for clinical applications in bone tissue engineering (Shi et al., 2016).

1.4.1.2.1 Gelatin (Gel)

Gelatin, a naturally derived polymer obtained by hydrolyzing collagen, has found widespread application in the field of 3D cell culture and tissue engineering. Its suitability arises from its unique properties, which provide the necessary chemical and biological cues for supporting diverse cell populations. This makes gelatin a valuable material for creating matrices for 3D cell culture and as a component of tissue-engineering scaffolds (Alipal et al., 2021). However, certain limitations associated with gelatin, such as its weak mechanical properties, rapid enzymatic degradation, and limited solubility in concentrated aqueous solutions, hinder its broader use. To overcome these limitations and enhance its performance, researchers have explored strategies such as combining gelatin with synthetic polymers like polycaprolactone (PCL), polyethylene glycol (PEG), and poly(lactic-co-glycolic acid) (PLGA). This allows for the creation of advanced biomaterials with tailored properties that can more effectively support cell growth, differentiation, and tissue regeneration (Afewerki et al., 2019).

1.4.1.2.2 Cellulose Acetate (CA)

Cellulose acetate (CA) is a biodegradable and biocompatible synthetic compound derived from the acetylation of natural cellulose (Janmohammadi et al., 2023). Its advantageous properties, including excellent chemical resistance, tunable mechanical strength, versatility in processing, and biodegradability, make it a promising candidate for scaffold materials in tissue engineering (Seddiqi et al., 2021). However, certain limitations need to be addressed before CA can be widely adopted in this field. Its limited thermal stability restricts its application in specific scenarios, and its mechanical strength, while tunable, can be insufficient for load-bearing applications (Seddiqi et al., 2021).

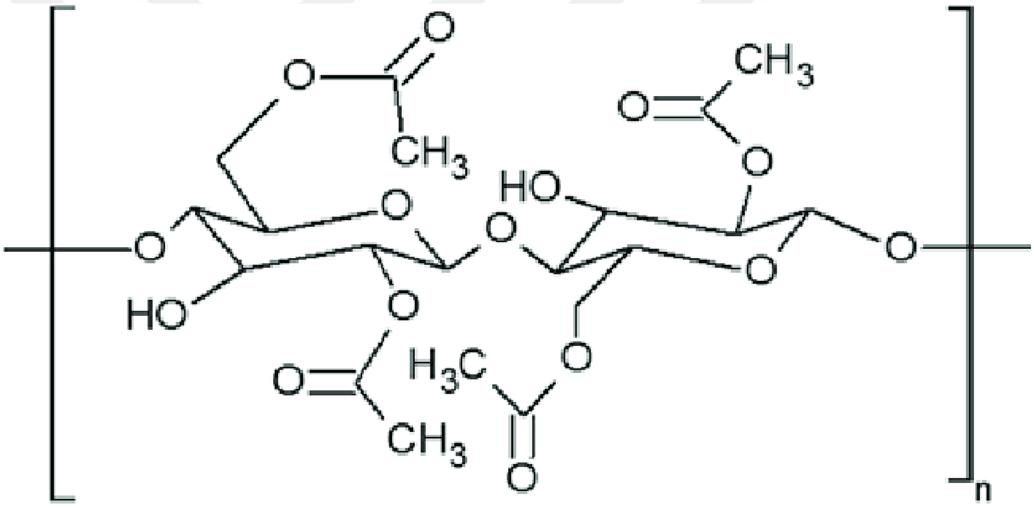

Figure 5. Chemical structure of CA (Janmohammadi et al., 2023).

1.4.2 Scaffold Production Methods in Bone Tissue Engineering

Methods used to produce scaffolds for bone tissue engineering can be classified as traditional methods and additive manufacturing methods.

Traditional methods use physical or chemical processes to create porous structures from biocompatible materials. Common traditional methods include:

i) Solvent casting/particulate leaching: A polymer solution is poured into a mold containing a porogen (such as salt or sugar). The solvent is then evaporated, leaving behind a nonporous scaffold. The porogen is then removed with a suitable solvent, leaving behind a porous scaffold with interconnected pores (Mikos et al., 1994; Nasr-Esfahani & Mehrabanian, 2011).

ii) Gas foaming: A polymer solution is saturated with a gas (such as carbon dioxide or nitrogen). The solution is then heated or depressurized, causing the gas to expand and create pores in the polymer. The gas then escapes, leaving behind a porous scaffold (Eltom et al., 2019a).

iii) Electrospinning: A high voltage is applied to a polymer solution, causing it to form a jet of nanofibers. The nanofibers are then collected on a collector to form a porous scaffold (Roseti et al., 2017).

iv)Freeze-drying: A polymer solution is frozen and then lyophilized (sublimated) to remove the ice. This leaves behind a porous scaffold with interconnected pores (Eltom et al., 2019b; Thavornyutikarn et al., 2014).

Additive manufacturing methods use computer-aided design (CAD) and computer-aided manufacturing (CAM) software to create three-dimensional (3D) objects from digital models. Common additive manufacturing methods used for scaffold production are:

Stereolithography (SLA): uses UV light to cure photo-sensitive resin, building structures layer-by-layer. Offers high resolution and detail, but requires specific resins and has limited material choices.

i. Fused deposition modeling (FDM): melts and extrudes a thermoplastic polymer filament to build structures layer-by-layer. Offers high porosity and ease of processing, but limited materials and requires high processing temperatures (Suamte et al., 2023).
ii. Selective laser sintering (SLS): uses a laser to sinter powder particles into solid structures layer-by-layer. Offers good mechanical strength and control over pore size and interconnectivity, but requires high temperatures and post-processing (Suamte et al., 2023).

iii. Binder jetting: deposits a binding agent onto a powder bed to selectively solidify layers, building the structure layer-by-layer. Offers low cost and rapid fabrication, but requires post-processing to remove unbound powder (Suamte et al., 2023).

iv. Inkjet printing: deposits droplets of biocompatible inks containing cells and materials onto a substrate. Offers high resolution and cell viability, but limited materials and potential for nozzle clogging (Suamte et al., 2023).

v. Laser-assisted bioprinting (LAB): uses a laser to create pressure pulses on a ribbon, ejecting bioink droplets to build structures layer-by-layer. Offers high cell viability and resolution, but requires specialized equipment (Suamte et al., 2023).

vi. Direct cell writing: extrudes a continuous filament containing cells and biomaterials through a micro nozzle to build structures layer-by-layer. Offers high cell density and compatibility with various materials, but limited resolution and potential for nozzle clogging (Suamte et al., 2023).

vii. Metal-based additive manufacturing: uses energy sources like laser or electron beam to melt and fuse metal powder into structures layer-by-layer. Offers patient-specific customization, and control over porosity and microstructure, but requires specialized equipment and expertise (Suamte et al., 2023).

1.5 Electrospinning

Electrospinning is a method for producing nanofibrous scaffolds with extremely thin fibers having diameters in the nanometer range. This method is versatile and scalable, so it can be used to produce nanofibers from a variety of materials and in large quantities. The process involves applying a high voltage to a polymer solution, which causes the solution to form a jet (Figure 6.). The jet then breaks up into a stream of nanofibers that are collected on a collector. Electrospun materials have a wide range of potential applications, including filtration, drug delivery, tissue engineering, energy storage, environmental remediation, and food packaging (Sharma et al., 2022).

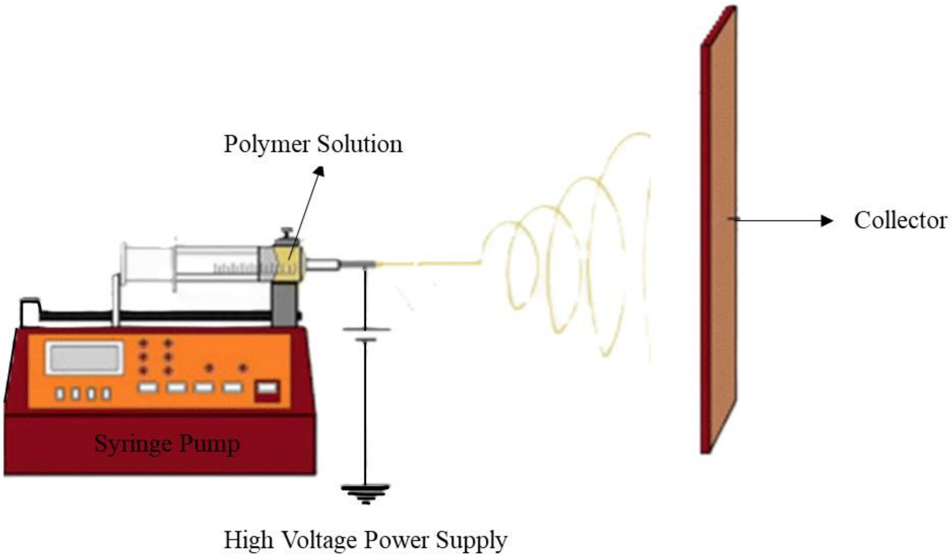

Figure 6. Illustration of electrospinning setup

As shown in Figure 6 an electrospinning setup typically consists of the A high voltage power supply that provides a high-voltage electric field to the polymer solution, which causes it to form a jet, a syringe pump that pumps the polymer solution through the needle or nozzle at a controlled rate, a needle or nozzle to dispenses the polymer solution into the electric field and a solid or liquid collector for collecting the electrospun nanofibers (Long et al., 2019).

1.5.1 Co-axial Electrospinning

Coaxial electrospinning stands as a sophisticated technique for producing nanofibers, characterized by their intricate morphologies and diverse functionalities. It represents an advancement over conventional electrospinning, where two or more polymer solutions are simultaneously extruded from a coaxial spinneret. The core solution resides within the inner capillary, while the shell solution encases it within the outer capillary. This unique arrangement enables the fabrication of nanofibers with a core-shell structure, allowing for the incorporation of diverse materials and functionalities (Pant et al., 2019; Qu et al., 2013).

Coaxial electrospinning offers several distinct advantages over its conventional counterpart, including:

- Fabrication of Core-Shell Nanofibers: Coaxial electrospinning facilitates the creation of nanofibers with a layered structure, enabling the encapsulation of materials and the controlled release of drugs or active agents (Pant et al., 2019; Qu et al., 2013).
- Enhanced Mechanical Properties: The core-shell structure imparted by coaxial electrospinning often results in nanofibers with improved mechanical properties, enhancing their durability and applicability (Pant et al., 2019; Qu et al., 2013).
- Tailored Release Profiles: Upon varying the core and sheath materials and thicknesses, coaxial electrospinning enables the fabrication of nanofibers with tailored release profiles, allowing for controlled release of drugs or active agents over extended periods (Pant et al., 2019; Qu et al., 2013).
- Enhanced Biocompatibility: The ability to incorporate biocompatible materials into the core or sheath of nanofibers enhances their biocompatibility and suitability for tissue engineering and biomedical applications (Pant et al., 2019; Qu et al., 2013).
- Versatility in Material Selection: Coaxial electrospinning accommodates a wide range of materials, including polymers, bioceramics, and metals, enabling the fabrication of nanofibers with diverse properties and functionalities (Pant et al., 2019; Qu et al., 2013).

In conclusion, coaxial electrospinning emerges as a powerful tool for fabricating nanofibers with intricate morphologies and differing functionalities, propelling advancements in various fields, including tissue engineering, drug delivery, biofiltration, sensor technology, and energy storage (Qu et al., 2013).

1.6 Challenges of Bone Tissue Engineering Approaches in Bone Healing

While bone tissue engineering holds immense potential, several key challenges impede its widespread application. These can be broadly categorized into fundamental, knowledge-related, evaluation, and clinical hurdles (Amini et al., 2012).

Table 1.2 Challenges of Bone Tissue Engineering

Fundamental Challenges	Component Selection: Determining the ideal combination of cell type, scaffold material with appropriate mechanical and porosity properties, and growth factors for each specific bone defect remains a significant challenge (Amini et al., 2012).
	Vascularization: Ensuring adequate and sustained blood flow throughout the engineered tissue is vital for its long-term survival and function, posing another critical hurdle (Maia et al., 2022).
	Host Integration: Seamless integration of the engineered bone with surrounding native tissue is crucial for optimal function and stability,

	presenting a major obstacle to overcome (Maia et al., 2022).
Knowledge-Related Challenges	Cell Contribution: Understanding the relative contributions of donor and host cells to bone regeneration is crucial for optimizing cell-based therapies (Amini et al., 2012).
	Immunomodulation: Developing effective strategies to suppress the immune response and prevent rejection of the engineered tissue is essential for successful bone tissue engineering (Amini et al., 2012).
	Side Effects and Complications: Carefully evaluating the potential side effects and complications related to various therapeutic agents used in bone tissue engineering is critical (Maia et al., 2022).
	Animal Models: Selecting the most appropriate animal models, particularly large animals that better represent human bone properties and healing, is crucial for pre-clinical testing (Amini et al., 2012; Maia et al., 2022).
	Bone Quality: An accurate assessment of the regenerated bone tissue's quality, including composition, structure, and

Evaluation Challenges	mechanical properties, is essential for evaluating its success (Amini et al., 2012; Maia et al., 2022).
	Bone Functionality: Assessing the functionality of the regenerated bone tissue, particularly its ability to withstand loads and support normal bone function, is vital for determining its effectiveness (Amini et al., 2012; Maia et al., 2022).
	Long-Term Tracking: Monitoring the long-term performance and stability of the engineered bone tissue over time is crucial for ensuring its long-term success (Amini et al., 2012; Maia et al., 2022).
Clinical Challenges	Regulatory Approval: Obtaining regulatory approval for clinical use of bone tissue engineering approaches, especially those involving multiple components or complex technologies, presents a significant hurdle (Amini et al., 2012; Maia et al., 2022).
	Multi-Component Strategies: Developing cost-effective and efficient methods for manufacturing and implementing multi-component bone tissue engineering strategies is essential for their clinical viability (Amini et al., 2012; Maia et al., 2022).

	Patient Specificity: The high cost associated with patient-specific bone tissue engineering approaches limits their accessibility and affordability (Amini et al., 2012; Maia et al., 2022).
	Alternatives to Patient-Specific Approaches: Exploring patient-independent methods for bone tissue engineering is crucial for increasing the accessibility and affordability of this technology (Amini et al., 2012; Maia et al., 2022).

1.6.1 Vascular Endothelial Growth Factor

Vascular endothelial growth factor (VEGF) is a signaling protein that plays a fundamental role in angiogenesis, the formation of new blood vessels, and vasculogenesis, the development of the initial blood vessel network during embryonic development (Ferrara, 2009). It promotes the differentiation of endothelial cell precursors and their assembly into functional blood vessels (Ferrara, 2004). Produced by a variety of cell types, including endothelial cells, macrophages, and platelets, VEGF exerts its effects by binding to two main receptors, VEGFR1 and VEGFR2, expressed on the surface of endothelial cells (Shibuya & Claesson-Welsh, 2006) VEGF is the most potent stimulator of angiogenesis known. It promotes the proliferation, migration, and survival of endothelial cells, the building blocks of blood vessels (Ferrara et al., 2003). VEGF increases vascular permeability, allowing fluid and macromolecules to leak out of blood vessels. This can be beneficial in some cases, such as wound healing, where it facilitates the delivery of immune cells and growth factors to the injured area (Ferrara, 2009). However, excessive vascular permeability can also be harmful, as seen in diabetic retinopathy, where it contributes to retinal edema and vision loss (Ferrara, 2004). VEGF has been implicated in neurogenesis, the formation of new neurons. Studies have shown that VEGF promotes the proliferation and survival of neural stem cells and enhances their differentiation into neurons (Ferrara, 2004). VEGF is a key factor in tumor growth and metastasis. It promotes angiogenesis, allowing tumors to develop new blood vessels to obtain oxygen and nutrients, which results in their growth and increased potential for spread (Ferrara, 2004).

Due to its critical roles in angiogenesis and vascular permeability, VEGF is involved in a variety of diseases such as cancer, diabetic retinopathy, age-related macular degeneration (AMD), rheumatoid arthritis (RA), and psoriasis (Ferrara, 2004). HIF1 Alpha and Its Role in Vascularization

1.6.2 HIF1 Alpha and Its Role in Vascularization

HIF-1α, a crucial transcriptional regulator, plays a pivotal role in cellular adaptation to low-oxygen environments. Under hypoxic conditions, HIF-1α stabilizes and binds with HIF-1β, activating the transcription of numerous genes involved in various cellular processes, including angiogenesis, metabolism, and cell survival (Semenza, 2003).

HIF-1α has emerged as a master regulator of angiogenesis, orchestrating a complex network of angiogenic factors and signaling pathways to promote the formation of new blood vessels (Semenza, 2010).

1.6.2.1 Mechanisms of HIF-1α-mediated Vascularization

HIF-1α regulates vascularization by inducing the expression of several pro-angiogenic factors, including vascular endothelial growth factor (VEGF), platelet-derived growth factor (PDGF), and angiopoietins. VEGF, a potent stimulator of endothelial cell proliferation and migration, is considered the primary mediator of HIF-1α-induced angiogenesis (Carmeliet & Jain, 2000).

Beyond its direct role in regulating angiogenic factors, HIF-1α also indirectly influences vascularization by modulating the expression of genes involved in cell metabolism, extracellular matrix remodeling, and immune cell recruitment (Semenza, 2010).

HIF-1α-mediated vascularization plays a critical role in various physiological and pathological processes:

-Embryonic development: HIF-1α is essential for proper vascular development during embryogenesis, ensuring adequate oxygen delivery to the growing embryo (Semenza, 2010).

-Wound healing: HIF-1α promotes angiogenesis during wound healing, facilitating the formation of new blood vessels to supply oxygen and nutrients to the healing tissue (Semenza, 2000).

-Tumor angiogenesis: HIF-1α is overexpressed in many types of tumors, where it contributes to tumor growth and metastasis by promoting angiogenesis (Semenza, 2010).

Vascular endothelial growth factor (VEGF) and hypoxia-inducible factor 1 alpha (HIF-1α) play pivotal roles in orchestrating angiogenesis, the intricate process of forming new blood vessels. Under normal oxygen conditions, HIF-1α undergoes rapid degradation. However, when oxygen levels decline (hypoxia), HIF-1α stabilization occurs, enabling its translocation to the nucleus. Within the nucleus, HIF-1α binds to hypoxia-response elements (HREs) located in the promoter regions of genes involved in angiogenesis, including VEGF. VEGF exerts a potent mitogenic effect on endothelial cells, the cellular constituents of blood vessel linings. It stimulates the proliferation, migration, and survival of endothelial cells, ultimately leading to the formation of new blood vessels. The intricate relationship between VEGF and HIF-1α is characterized by bidirectional signaling. HIF-1α induces VEGF expression, and in turn, VEGF contributes to HIF-1α stabilization. This positive feedback loop ensures that angiogenesis is effectively activated under hypoxic conditions when it is most crucial. Dysregulation of the VEGF-HIF-1α pathway is implicated in a wide spectrum of diseases, encompassing cancer, cardiovascular diseases, and inflammatory disorders. In the context of cancer, tumor cells frequently secrete elevated levels of VEGF, which can stimulate the growth of new blood vessels, providing the tumor with essential oxygen and nutrients (Forsythe et al., 1996; Semenza, 2003).

1.6.3 Hormones Involved in Bone Growth and Regeneration

Hormones are signaling molecules produced by endocrine glands and travel through the bloodstream to exert their effects on target tissues. Some hormones play a role in bone healing by regulating the overall metabolic environment and coordinating the activities of different cell types, some hormones may directly act on Bone cells for their purpose. Some of the key hormones involved in bone healing include:

- Parathyroid hormone (PTH): PTH regulates calcium levels in the blood and by affecting bone cells stimulates bone remodeling, promoting the breakdown of old bone and the formation of new bone (Marsell & Einhorn, 2011).
- Vitamin D: Vitamin D enhances calcium absorption from the intestines and is essential for bone mineralization, the process by which bone tissue becomes hardened (Dimitriou et al., 2011).
- Growth hormone (GH): GH is responsible for overall growth and development. It also contributes to bone growth and healing by stimulating the production of IGF-1 (Einhorn, 1996).

The understanding of the role of growth factors and hormones in bone healing has led to the development of new therapeutic approaches for treating fractures and other bone injuries. These approaches either local application of growth factors in which growth factors can be applied directly to the fracture site to promote bone healing using a variety of methods, such as injections, gels, and scaffolds (Sheikh et al., 2015) or by Systemic administration of hormones that is typically done with medications that mimic the effects of natural hormones (Sheikh et al., 2015).

These therapeutic approaches have shown promise in clinical trials and are now being used to treat patients with a variety of bone injuries.

In recent years there were new studies on another hormone, Ghrelin. Ghrelin, an orexigenic hormone primarily produced by the stomach, has emerged as a potential therapeutic agent in bone tissue engineering due to its multifaceted effects on bone metabolism. Studies have demonstrated that ghrelin directly stimulates osteoblast proliferation, differentiation, and mineralization, leading to enhanced bone formation (Fukushima et al., 2005; Kim et al., 2005a). Additionally, ghrelin promotes angiogenesis, the formation of new blood vessels, which is crucial for bone regeneration (L. Wang et al., 2012). Furthermore, ghrelin has anti-inflammatory properties, which can contribute to a favorable environment for bone healing (Delhanty et al., 2014).

Ghrelin exerts its effects on bone cells through the growth hormone secretagogue receptor (GHS-R), which is expressed in osteoblasts, osteoclasts, and bone marrow stromal cells (Delhanty et al., 2014). Activation of GHS-R by ghrelin triggers a signaling cascade involving mitogen-activated protein kinases (MAPKs) and phosphatidylinositol 3-kinase (PI3K) /Akt pathways, leading to the upregulation of bone-forming genes and the suppression of bone-resorbing genes (Kim et al., 2005b).

Ghrelin administration has been shown to promote bone healing in animal models of fracture and osteoporosis. In a study by Erener et al., ghrelin treatment significantly accelerated bone fracture healing in rats, with increased bone mass, callus formation, and bone mineral density (Erener et al., 2021).

The potential therapeutic application of ghrelin in bone tissue engineering is further supported by its ability to enhance the osteogenic potential of mesenchymal stem cells (MSCs), which are multipotent cells that can differentiate into various cell types, including osteoblasts. Ghrelin treatment has been shown to increase the proliferation, differentiation, and mineralization of

MSCs, suggesting its potential to promote bone regeneration in vitro and in vivo (Barre et al., 2020; L. Wang et al., 2012).

1.7 Aim of The Study

Inbone tissue engineering, as of the main challanges onsuccess, it is proosed that the tissue scaffold should support osteogenesis while also supporting angiogenesis. The use of stem cells and growth factors, which are the most suitable solution approaches for this purpose, also have unique restrictions and problems. Therefore, the main purpose in this thesis is to develop a new bone tissue engineering scaffold biomaterial that will support regeneration and angiogenesis by providing the necessary pathways with local controlled release of a peptide hormone (ghrelin), and a transcription factor (HIF-1 α), besides a being suitable for cell adhesion and proliferation.

Considering the studies in the literature developed scaffold was designed with the aim to prevent the failure of the treatment due to the fact that osteogenesis starts immediately after the damage but angiogenesis starts later. Thus,to develop a bone tissue scaffold that can support the angiogenesis with the early release of the HIF1-α protein from the shell layer of the fibers of 3D tissue scaffold and the long-term and controlled release of Ghrelin from the core layers of the fibers.

The materials selected for the production of tissue scaffolds are very important in terms of providing osteoinductive niches for cells and the rate of degradation. In the literature research, natural and synthetic polymers were investigated. In this thesis, cellulose acetate, which is biocompatible, biodegradable, and has regenerative properties, is chosen as the shell layer for the fibers in the tissue scaffolds to be created. In addition, it has been observed that molecules loaded on cellulose acetate exhibit an immediate release profile in the literature studies. Since it is desired for the rapid release of HIF1-α , it was loaded to cellulose acetate as outer layer (shell) of the fibers. PCL is a hydrophobic material and is therefore often preferred in controlled drug delivery systems. On the other hand, gelatin is a highly hydrophilic material. Therefore, PCL was preferred to be used together with gelatin to modify the degradation rate of PCL as the core layer material of the fibers of scaffold to create a slow and longer-term release profile for ghrelin. In this thesis, a study on the controlled release of the ghrelinand HIF1-α were conducted for the first time. As a result of the literature reviews, as far as we know, tissue scaffold with these polymer compositions and organizations was realized firstly in this thesis using the coaxial electrospinning method by using PCL, gelatin, and cellulose acetate polymers together.

CHAPTER 2

MATERIAL AND METHODS

2.1 Materials

Cellulose acetate (CA, 39.8 wt. % acetyl, Mw=30,000 by GPC), gelatin from porcine skin (gel strength 300, Type A), and Polycaprolactone (PCL, Mw:80000), sodium carbonate (Na_2CO_3,), sodium bicarbonate ($NaHCO_3$,), cupric sulfate ($CuSO_{4}.5H_2O$), 4-Nitrophenyl phosphate (pNPP) and bicinchoninic acid solution (BCA) were purchased from Sigma-Aldrich (Germany). Hexafluro-2-propanol (HFIP) from Interlab (Turkey) was used as a solvent for electrospinning of all polymers. Human Hypoxia-inducible Factor 1 Alpha (HIF 1A) and recombinant Ghrelin (GHRL) proteins were obtained from Prospec (Israel). HIF 1A ELISA (Enzyme-Linked Immuno Sorbent Assay), Ghrelin ELISA, and VEGF ELISA kits were purchased from BT LAB (China). HUVEC basal media was Sigma-Aldrich (Germany), supplement from Zeydanlı (Turkey), Dulbecco's Modified Eagle Medium F12 (DMEM F12), Fetal bovine serum (FBS) from Serox (Turkey) were bought for cell culture experiments.

2.2 Methods

2.2.1 Composition of Polymer Solutions for Single Electrospinning

To find a suitable solvent sytem for CA and PCL-Gel solutions, optimization studes with solvents in Table 2.1 were carried out. The polymer solutions were prepared at room temperature and stirred at 400 rpm with a magnetic stirrer.

Table 2.1 The list of solvents and concentrations tested.

Polymer	Solution	Solvent Ratio	Polymer Concentration	Polymer Ratio
PCL-Gel	AA/FA	9:1 v,v	20% w,v	50:50(w, w)
PCL-Gel	$CHCl_3$/ MeOH	3:1 v,v	%20% PCL	4:1 (v,v)
	CH_3COCH_3/dH_2O	4:1 v,v	8% Gel	
PCL-Gel	HFIP	-	10%	80:20
PCL-Gel	HFIP	-	12%	80:20
PCL-Gel	HFIP	-	15%	50:50
PCL-Gel	HFIP	-	20%	50:50
CA	Aceton	-	8%	-
CA	Acetone	-	12.5%	-
CA	Acetone/DMac	3:1 v,v	4%	-
CA	Acetone/DMac	3:1 v,v	6%	-
CA	Acetone/DMac	50:50 v,v	16%	-
CA	Acetone/DMac	70:30 v,v	16%	-
CA	Acetone/DMac	3:1 v,v	16%	-
CA	DCM/Acetone	3:1 v,v	7.5%	-
CA	DCM/Acetone	3:1 v,v	10%	-
CA	AA/ dH_2O	75:25 v,v	17%	-

CA	AA/ dH_2O	3:1 v,v	18%	-
CA	AA/ dH_2O	2:1 v,v	15%	-
CA	AA/ dH_2O	4:1 v,v	17%	-
CA	Acetone/DCM/DMF	2:1:1 v,v,v	12%	-

2.2.2 Compositions of Polymer Solutions for Coaxial Electrospinning

Hexafluoroisopropanol (HFIP) was used as the solvent for all three polymers; cellulose, gelatin, and PCL. For optimization studies, PCL-GEL solutions at ratios of 70:30 and 80:20 (w/w PCL-Gel) with a total polymer concentration of PCL-Gel solution of 10% (w/v) were prepared to be used in the inner (core) fiber phase along with CA solutions at concentrations of 10%, 15%, and 20% (w/v) for the outer (Shell) fibers.

2.2.3 Coaxial Electrospinning for 3-D Fibrous Scaffold Production

The setup utilized for wet co-axial electrospinning comprised of two NE-1000 syringe pumps (New Era Pump Systems, Inc. USA), an ES30 Gamma High Voltage Source (Gamma High Voltage Research, Inc. USA), an immobile metal collector, a rotating collector stand (Gözeler Elektronik, Turkey), and a plexiglass cabinet (Kesit Pleksi, Turkey).

The configuration was adjusted to a vertical orientation, leveraging gravitational forces to augment jet formation along its trajectory. The rotational collector stand was positioned at the lower section of the enclosure. The formed fibers accumulated in a petri dish containing 100% absolute ethanol, positioned on this collector as shown in Figure 7.

For optimization studies, voltage values ranging from 5 to 22 kV and distance values between 5 and 10 cm were tried. To determine the optimal solution concentration, scaffolds were produced with each solution via their single electrospinning. Subsequently, scaffolds with core-shell fiber structure were produced as shown in Table 2.2 using co-axial wet electrospinning at the determined concentrations.

Table 2.2. Groups of scaffold (%10 PCL-Gel (8:2), %12 CA, 22kV, 8 cm, 1/5mL/h (PCL-Gel/CA), ethanol)

Number	Groups
1	PCL-GEL/CA (without Ghrelin and HIF1 alpha)
2	Ghrelin-PCL-GEL/CA (without HIF1 alpha)
3	PCL-GEL/CA-HIF1 alpha (without Ghrelin)

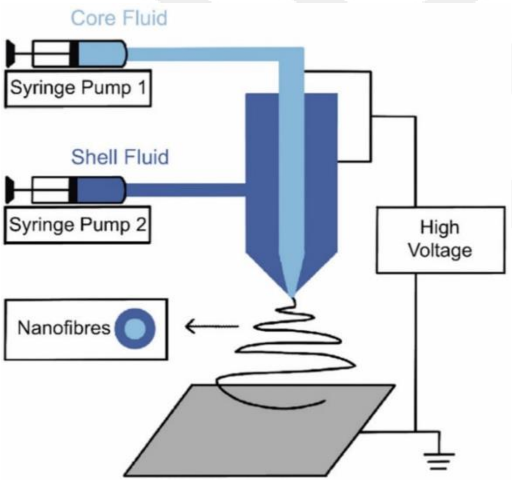

Figure 7. Co-axial electrospinning setup (Han & Steckl, 2019).

To obtain scaffolds loaded with two proteins; HIF-1 alpha (5000 ng) and Ghrelin (5000 ng), They were added to polymer solutions and mixed with a a magnetic stirrer. According to the purpose of use of these proteins for enhancement of Bone regeneration capacity of the scaffolds HIF-1 alpha was added to cellulose asetate solution that will be for the shell and ghrelin protein was added to PCL-GEL solution that will make the core of the fibers. The scaffolds were obtained by spinning these solutions according to the above settings. Subsequently, the electrospun scaffolds were lyophilized using a freeze-drier (Labconco Corporation

USA) following freezing at a temperature of -80°C refrigerator (Nuaire, USA). After freeze-drying, all scaffolds were stored at -20 °C.

2.2.4 Characterization of Scaffolds

2.2.4.1. Scanning Electron Microscopy (SEM) Analysis

The morphology and structural characteristics of electrospun scaffolds were assessed through scanning electron microscopy (SEM). Samples were prepared for analysis by coating with a layer of gold using a sputter coating apparatus. The fibrous structures were scrutinized utilizing SEM devices (FEI Quanta FEG SEM 650, USA), in the Center of Biomaterials and Tissue Engineering (BIOMATEN) at METU, Turkey. Fiber morphologies and distributions of fiber diameters of scaffolds were examined from images obtained from different areas on the scaffolds.

2.2.4.2. Degradation and Swelling Experiments of Scaffolds

In degradation experiments, scaffolds were cut to have similar weights with avg:15mg±2 mg. Separate sets of samples were prepared for each time point of degradation experiments. Each sample was immersed in a 5 ml solution of phosphate-buffered saline (PBS, 0.1 M, pH: 7.4) and incubated at 37°C while stirring at 66 rpm in a water bath (Nüve Bath NB, Turkey) for 14 days. The samples were collected at predetermined time points, washed with distilled water, and first, their wet weights were measured for evaluation of water holding property. Subsequently, they underwent lyophilization using a freeze-drier (from Labconco Corporation located in Kansas City, USA), following freezing at a temperature of -80°C for measurements of dry weights at the end of the 1st, 7th, and 14th days. To quantify the weight loss, we applied the formula provided below:

$$\text{Weight loss (\%)} = \frac{W_0 - W_1}{W_0} \text{ x } 100$$

W_0: Initial dry weight of the scaffold

W_1: Dry weight of the scaffold at each time point

Swelling (%) = $\frac{W_1 - W_0}{W_0}$ x 100

W_0: Initial dry weight of the scaffold

W_1: Wet weight of the scaffold at each time point

2. 2. 4. 3. Creating a Calibration Curve for Proteins

HIF1 a was prepared in PBS to final concentrations of 8, 4, 2, 1, and 0.5 ng/ml. Also, ghrelin was prepared in PBS to final concentrations of 0.78, 1.56, 3.17, 6.25, 12.5, 35, 50,70, and 100. The prepared samples and PBS were scanned over a 600-190 nm wavelength via a spectrophotometer (Molecular Devices, USA).

OD correction = $OD_{protein}$- OD_{PBS}

2. 2. 4. 4. Protein Loading and Release Experiments

A wavelength scan was performed to create a calibration curve for ghrelin and HIF1-ɑ because of elisa kit failure. PBS was used as the background in the experiment. Figures 20, 21, and 22 at appendices show the absorbance graphs obtained at the highest protein concentrations and the absorbance graphs obtained for PBS. The absorbance values obtained for proteins from the wavelength scan were subtracted from the absorbance value of PBS. Consistent results were obtained at 220 nm wavelength for HIF1a, and at 200 nm wavelength for ghrelin.

Photons with a wavelength maximum shorter than 210 nm are absorbed by the peptide bond. Nonetheless, there may be advantages in terms of instrumentation and measurement sensitivity when determining the peptide bond's broad absorption peak at longer wavelengths. Absorbance at 214 and 220 nm is frequently used as an alternative to 210 nm when measuring proteins and peptides due to the possible interference of components in biological buffers and solvents. Proteins with a high number of peptide bonds can improve the accuracy of Abs205 nm measurements and show less variation between proteins than Abs280 nm measurements.

Different scaffolds were prepared with the compositions given in Table 2.3 samples weighing 10 mg (scaffold loaded with HIF1-ɑ) and 2.6 (scaffold loaded with Ghrelin) were taken from the scaffolds and placed in sealed tubes containing 5 ml of PBS (0.01 mM, pH 7.4 with 0.022% Sodium Azide). These tubes were then left in a water bath at 37°C for 7 days (Nüve ST30, Turkey). To determine HIF1-ɑ and Ghrelin release amounts, samples were collected at time points: Day 1, 3, and 7. The results of the release samples were cumulatively calcuulated according to the equation provided below:

Cumulative release amount (%) = $\sum \left(\frac{M(i)}{M(0)}\right) x\ 100,$

$M_{(i)}$: The quantity of Protein-Peptide determined at each measurement point

$M_{(0)}$: The initially loaded amount of Proteins HIF 1 Alpha and Ghrelin Release

2. 2. 4. 5. Cell Attachment Properties of Scaffold

After 1, 3, and 7 days of incubation, the attachment properties of the cells on the scaffolds were investigated using an SEM (Quanta 200 FEG, The Netherlands). Cells were fixed in 4% paraformaldehyde solution in PBS after each period. Before being stored in a refrigerator, fixed samples were first cleaned with PBS, then dried in hexamethyldisilazane for 20 minutes. Dehydration was achieved by gradually increasing the ethanol series (50–100%). Before SEM analysis, batches were imaged using scanning electron microscopy (Stereoscan S4-10, Cambridge, UK, and JSM-6400 Electron Microscope, Jeol Ltd., UK), which was outfitted with NORAN System 6 X-ray Microanalysis System & Semafore Digitizer (Thermo Fisher Scientific Inc., USA). The batches were coated with an ultrafine (10 nm) gold layer using a precision etching coating system (682 PECS, Gatan, Inc., USA).

2.2.5 Cell Culture Studies

For the cell culture experiments, the human fetal osteoblast (hFOB) cell line and human umbilical cord vein endothelial cells (HUVEC) were used. HFOB was cultured in a growth medium consisting of DMEM/F-12 nutrient medium, supplemented with 10% (v/v) fetal bovine serum (FBS) and 5% penicillin-streptomycin and L-glutamine. HUVEC was cultured in a growth medium (Endogo XF Basal Medium) consisting of 0.5% supplement (Endogo XF Supplement Mix). The cell culture was maintained at 37°C in a 5% CO_2 atmosphere within a carbon dioxide incubator (5215 Shel Lab., Cornelius, OR, USA). Once they reached 80% confluency, the cells were subcultured using a 0.1% Trypsin/EDTA solution. The experiments utilized HFOB in the 4^{th} and HUVEC in the 5^{th} passage.

Before conducting in vitro cell culture experiments, the scaffolds were sterilized. This was achieved by exposing them to UV irradiation for 30 minutes for each site.

2.2.5.1 Ghrelin Dose Studies

To determine the effective dose of Ghrelin on Bone cells, Ghrelin dose-response studies were conducted. Ghrelin solutions were prepared at the concentrations specified which were 1, 5, 10,20, and 40 nM. For dose experiments, 10 000 HFOB cells (n=3) were seeded to each well of 96-well plates, and 250 µL of growth media was added. After incubating for one day at 37°C, the cell media was collected and the wells were washed with sterile PBS. Then DMEM F12 media involving different amounts of Ghrelin were added to the wells, and the total media volume was adjusted to 250 µl to achieve the final doses of Ghrelin mentioned above. The cells were incubated with Ghrelin for one day in a carbon dioxide incubator.

At the end of 24 hours and 3 days, media was collected from the cells, and 100 µL of Alamar Blue, diluted in DMEM without phenol red (at a concentration of 10%), was added. The results were recorded at 570 nm and 600 nm via microplate spectrophotometer (µOuantTM, Biotek Instruments Inc., USA) after 4 hours of incubation at 37°C. (Please refer to sec. 2.2.4.3 Cell viability.)

After the 7th and 14th days of Ghrelin exposure, an alkaline phosphatase assay was performed on the cells to examine osteogenic differentiation. (Please refer to sec. 2.2.4.4 Alkaline phosphatase activity.)

2.2.5.2 HIF1 Alpha Dose Studies

To determine the effective quantity of HIF-1 alpha on endothelial cells, 10000 HUVEC cells were seeded to each well of a 96-well plate, and 250 µL HUVEC basal media was added. After a one-day incubation at 37 °C, the media was removed from the cells and replaced with a new 250 µL solution containing a mixture of HIF1-α and HUVEC media diluted with basal media to obtain final HIF1-α concentrations of 2, 8, 16, and 32 ng/ml.

The cells were then cultured for 24 hours at 37°C in a CO2 incubator. At the end of 24-hour and 48-hour periods, the media were collected from each well to examine the VEGF levels via ELISA kit according to the kits' protocol. Additionally, cell viability was assessed at 24 and 48 hours using the Alamar Blue assay. (Please refer to sec. 2.2.4.3 Cell viability.)

2.2.5.3 Cell Viability

For cell viability, Alamar Blue was diluted with phenol-red-free DMEM to a concentration of 10%.

In the dose-response experiments, 24 and 72 hours after providing Ghrelin to HFOB cells and 24 and 48 hours after giving HIF-1 alpha to HUVEC cells, the media on top of the cells were collected, and 100 µL of Alamar Blue was added. The cells were then incubated with Alamar Blue for 4 hours at 37°C in an incubator containing 5% atmospheric CO_2. Following this, absorbance readings were taken using a microplate reader (µQuant, BioTek®, Winooski, VT, USA) at primary and reference wavelengths of 570 nm and 600 nm, respectively. The results were analyzed according to the formula provided below.

Percentage reduction of AlamarBlue = $\frac{(\mathrm{O}(\prime) x A(1))-(O(1) x A(2))}{(R(1) x N(2))-(R(2) x N(1))}\ x\ 100$

O(1): Molar extinction coefficient of oxidized AlamarBlue (blue) at 570 nm

O(2): Molar extinction coefficient of oxidized AlamarBlue (blue) at 600 nm

R1 = Molar extinction coefficient of reduced alamarBlue (red) at 570 nm

R2 = Molar extinction coefficient of reduced AlamarBlue (red) at 600 nm

A1 = Absorbance of test wells at 570 nm

A2 = Absorbance of test wells at 600 nm

N1 = Absorbance of negative control well (media plus alamarBlue but no cells) at 570 nm

N2 = Absorbance of negative control well (media plus alamarBlue but no cells) at 600 nm

2.2.5.4 Alkaline Phosphatase Activity

After exposing ghrelin for 7 days, media is collected from the cells, and the well plates are washed with phosphate buffer saline solution (PBS). Then, 200 µL of lysis buffer (bursting solution) is added to the cells, and they are placed at -80°C. The frozen well plates are rapidly thawed with hot water to burst the cells. The burst cells from each well are transferred to Eppendorf tubes, and the tubes are centrifuged at 8000 rpm for 5 minutes to precipitate cell residues. The liquid remaining above the Eppendorfs (50 µL) is taken and transferred to 48-well cell plates. To these, 350 µL of bicinchoninic acid working solution (BCA) is added, and they are incubated at 37°C for 30 minutes before measuring at 562 nm wavelength.

50 µL from the Eppendorf is transferred to a 96-well cell plate, mixed with 100 µL of PNPP, and incubated at 37°C for 60 minutes before measuring at 405 nm wavelength. The enzyme activity of the cells is calculated as uMol (ALP)/g Protein (BCA).

To prepare 0.2 M carbonate buffer, 4.240 g of sodium carbonate (Na_2CO_3: M_w=105.99 g/mol; ρ=2.54 g/cm³) was dissolved in 200 ml of distilled water (dH_2O). A different beaker dissolved 1.680 g of sodium bicarbonate ($NaHCO_3$; Mw=84.01 g/mol; ρ=2.2 g/cm³) in 100 ml of dH_2O. Afterward, the sodium bicarbonate solution was mixed with the 200 ml sodium carbonate mixture. To achieve a pH level of 10.2 for the carbonate buffer, NaOH (1M) was added to the mixture last.

To create a 0.1% Triton X 100 solution, Triton X 100 was blended with distilled water. To formulate the burst solution, a mixture of 1% Triton X 100 and carbonate buffer in a 1:9 ratio was prepared.

To make a 100 mM Mg-Cl solution, 0.203 g of magnesium chloride hexahydrate ($MgCl_2 \cdot 6H_2O$; M_w=203.3 g/mol) was thoroughly mixed in 10 ml of distilled water using vortex.

The PNPP working solution is prepared by mixing PNPP substrate solution, Magnesium-Chlorine solution, and dH2O in a ratio of 10:1:20 (v:v:v).

To obtain the bicinchoninic acid working solution, bicinchoninic acid is mixed with 4% cubric sulfate in a 50:1 (v:v) ratio.

2.2.5.5 Evaluation of Ghrelin and HIF1Alpha loaded PCL-GEL/CA Scaffolds for In vitro Angiogenesis and Osteogenes Properties

For angiogenesis studies, 10 mg (n=3) of tissue scaffolds loaded with i) only HIF1 alpha in the shell, and ii) protein-free scaffolds were used. Those samples were put into ethanol (%70) for 1 hour and then they washed twice with sterile PBS. Sterilized tissue scaffolds were placed in 96-well cell culture plates and incubated into 250 uL huvec media for 1 day at 37 ℃. At the same time, 10.000 HUVEC cells were seeded in a 96-well cell culture plate and incubated for 1 day at 37 ℃. After 1 day media which was incubated with scaffolds transferred Huvec cell. Media from the wells were collected on the 1st, 3rd, and 7th days, and VEGF levels were measured via ELISA kit.

For osteogenic differentiation, 10 mg (n=3) of tissue scaffolds loaded with i) only Ghrelin in the core, and ii) protein-free scaffold were examined. Sterilized tissue scaffolds were placed in 96-well cell culture plates and incubated into 250 uL HFOB media for 1 day at 37 ℃. At the same time, 10.000 HFOB cells were seeded in a 96-well cell culture plate and incubated for 1 day at 37 ℃. After 1 day media which was incubated with scaffolds transferred HFOB cell. ALP activity was measured on the 7th and 14th days to calculate and compare osteogenic differentiation enzyme activities. (Please refer to sec. 2.2.4.4 Alkaline phosphatase activity.)

2.2.6 Statistical Analysis

Statistical analysis of the data was conducted using SPSS software (version 23.0; IBM Corporation, NY, USA) with One-Way Analysis of Variance (ANOVA) and Tukey's post hoc test for multiple comparisons. Statistical significance was determined at $p \leq 0.05$, and the results were presented as the mean ± standard deviation (SD).

CHAPTER 3

RESULTS AND DISCUSSION

3.1 Electrospun Scaffold Production and Characterization

3.1.1 Optimization of Solvent System for PCL-GEL and CA

In order to obtain scaffolds with double-layered (Core/Shell) fibers (by coaxial electrospinning, first optimizations of core and shell components as single fiber forms were done using various solvent systems.

Polycaprolactone (PCL) and gelatin (GEL) polymers are selected to be used in the core layer owing to specific properties of theese polymers compatible with the aim of the study. PCL is a synthetic polymer that is biocompatible, and biodegradable providing good control on the release of drug/bioactive agents due to its hydrophobicity. However, it lacks specific cell recognition domains and it is degrading slowly even in in vivo conditions. To overcome these limitations and reduce the degradation time, it is often mixed with natural polymers such as gelatin or collagen. Various solvents and solvent combinations were tried to prepare PCL-Gel solutions. Here, results showed that the major problem of the solvent systems used in the PCL/Gel solution was the inability to obtain a homogeneous solution. Upon testing these solvents (Table 2.1), best complete dissolution of both polymers was achieved with HFIP which provided a homogeneous solution. HFIP or TFE (trifluoroethanol) are generally preferred solvents in PCL like highly hydrophobic synthetic or natural polymers (Jeong et al., 2008). In a study by Zhang et al, HFIP and TFE solvents were suggested as the best option because homogeneous dissolution could not be achieved with other organic solvents (Zhang et al., 2007).

The Shell layer component was decided as cellulose acetate which is also a commonly used polymer in in tissue engineering studies due to its being biocompatible and biodegradable (Angel et al., 2020). The main problem encountered in optimizations study of the cellulose acetate polymer electrospinning part was the failure of most of its good solvents in electrospinning trials.

In CA solutions using acetone, the needle tips were constantly clogged by rapid evaporation of the solvent. Scaffolds could not be obtained in acetic acid because the solvent evaporated quickly. When acetone and DCM were used, excessively viscous solutions were obtained and thus, clogging occurred at the needle tip. When the solvent system of DMSO and DMac were applied, fibers were excessively brittle, thus, continuous fibers were not obtained in wet electrospinning. In solutions using HFIP, no fibers could be produced with 20% polymer concentration but 15% and 12% cellulose acetate concentrations of HFIP gave positive and similar results. There has been some debate concerning the creation of CA fibers in which acetone is the only solvent used. Continuous fibers could not be produced by CA in solitary acetone, according to reports by Liu and Hsieh and Tungprapa et al (Liu & Hsieh, 2002; Rodríguez et al., 2012; Tungprapa et al., 2007). To facilitate the synthesis of CA nanofibers, an additional solvent may need to be added, according to both studies. Tungprapa et al. look into the inclusion of DMAc, which is suggested by Liu and Hsieh (Liu & Hsieh, 2002; Rodríguez et al., 2012; Tungprapa et al., 2007). Son et al. showed that CA can be spun with success utilizing a water-acetone mixed solvent system, with 10% and 15% (w/w) being the ideal water content (Son et al., 2004; Tungprapa et al., 2007)

In conclusion, HFIP was the only solvent that could produce a homogeneous solution for PCL-Gel among the solvent systems and provided good solubity and electrospinnability for CA polymer. Additionally, it was thought that in the coaxial electrospinning method, using the same solvent in the core and shell solution helps to reduce the interfacial tension, which supports the development of a uniform core-shell fiber (Yu et al., 2004). Due to the problems experienced with other solvents selected for CA, as well as to reduce the surface interfacial tension between the two solutions in coaxial electrospinning, it was decided to use HFIP as the solvent for both the core and shell solutions.

3.1.2 Optimization and Characterization of Wet Electrospinning Process to Obtain PCL-Gel/CA Scaffolds

To find the optimal coaxial electrospinning parameters (voltage, flow rate, distance, and collector) with the selected solvent, single electrospinning experiments were performed using solutions with different concentrations of the core and shell components separately. In optimization experiments; the flow rate was in the interval of 0.01-9 mL/h, the distance was between 5-12 cm, the voltage range was 8-22 kV, and water, water+tween80, and ethanol were tested as collection media of wet electrospinning. First, the shell phase component, CA was optimized for electrospinning parameters. When 10% CA solution was collected for 15 minutes at 1 mL/h and 5 mL/h flow rates, 15-18 kV voltage range, and using tween80+water collector set at 8 and 12 cm distances, brittle fibers were obtained in all conditions. The 10% CA mixture was durable enough to be collected at a flow rate of 5 mL/h under 18-20 kV voltage at a distance of 5 cm. The reason for this is thought to be that the voltage and surface tension applied to low-concentration solutions cause breaks in the polymer fiber before it reaches the collector. No fiber production occurred for the 20% CA solution because of its' viscosity which was also reported in literature as high solution concentrations, the solution can block the flow from the needle tip and dry there, causing clogging in the needle (S. Haider et al., 2013). In the 15% CA solution, 3-D scaffolds could be collected at three collection media; ethanol, water, and tween80+water (using flow rates: at 10 cm, 22-18 kV, and 1-9 mL/h, respectively) and SEM analysis could be performed (Figure 8). In Figure 8. A, B, C, D, and G, no beads were observed, and continuous fibers could be produced. Although a smooth fiber structure was obtained in the experiment with water (Figure 8 G) it was not preferred because it might dissolve the peptide/protein molecules loaded in final form.

Table 3.1 Experiment groups and parameters used in optimization studies of electrospinning of CA.

Sample	**Concentration**	**Paramaters**	**Collector**	**Result**
CA+HFIP	15%	9 mL/h, 22 kV, 10 cm	Ethanol	Good fiber
CA+HFIP	15%	9 mL/h, 18 kV, 10 cm	Ethanol	Good fiber
CA+HFIP	15%	5 mL/h, 22 kV, 10 cm	Ethanol	Good fiber
CA+HFIP	15%	5 mL/h, 18 kV, 10 cm	Ethanol	Good fiber
CA+HFIP	15%	9 mL/h, 22 kV, 10 cm	Tween80+H_2O	Fused fiber
CA+HFIP	15%	5 mL/h, 18 kV, 10 cm	Tween80+H_2O	Fused fiber
CA+HFIP	15%	1 mL/h, 18 kV, 10 cm	H_2O	Not choosen because of proteins

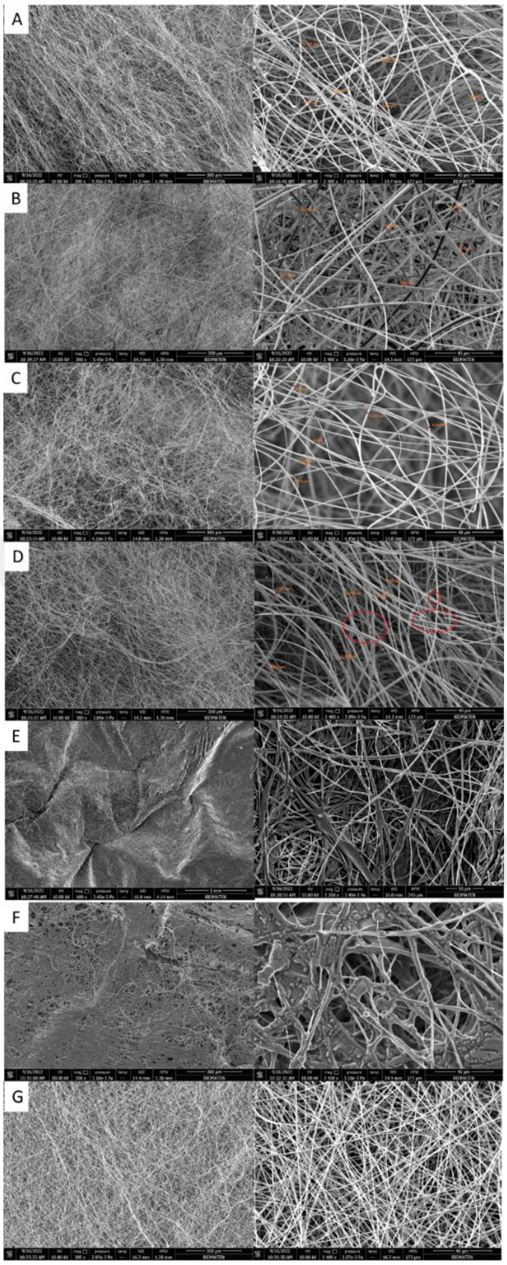

Figure 8. SEM images at 300x (left) and 2400x (right) of (A) CA in ethanol (15% w,v, 22 kV, 9 mL/h, 10 cm), (B) CA in ethanol (15% w,v, 18 kV, 9 mL/h, 10 cm)(C) CA in ethanol (15% w,v, 22 kV, 5 mL/h, 10 cm), (D) CA in ethanol (15% w,v, 18 kV, 5 mL/h, 10 cm), (E) CA in Tween80+sH_2O (15% w,v, 22 kV, 9 mL/h, 10 cm), (F) CA in Tween80+sH_2O (15% w,v, 18 kV, 5 mL/h, 10 cm), (G) CA in dH_2O (15% w,v, 18 kV, 1mL/h, 10 cm.

Table 3.2 Figure 8. A, B, C, and D scaffolds fiber diameter measurements (performed using ImageJ).

Sample	Min Value (µm)	Max Value (µm)	Average (µm)	Standard Deviation (µm)
A	0.71	1.76	1.25	0.32
B	0.33	0.64	0.44	0.11
C	0.34	0.86	0.51	0.15
D	0.36	0.86	0.45	0.14

In the electrospinning method, the current from the voltage source is transferred to the solution with a metal needle, forming a spherical Taylor cone, thus producing nanofibers. The critical voltage level required for the formation of a Taylor cone varies from polymer to polymer (A. Haider et al., 2018) . According to Deitzel et al., nanofibers with smaller diameters are formed with increasing voltage (Deitzel et al., 2001) . On the other hand, a voltage increase can also lead to an increase in the diameter of the nanofibers due to the formation of a longer Taylor cone (Baumgarten, 1971). Another parameter that affects fiber morphology is flow rate. As the flow rate increases (as long as it does not exceed the critical level), the fiber diameter increases. As the flow rate exceeds the critical level, bead-like structures or ribbon-like fibers are observed (A. Haider et al., 2018). When Figure 8. A and C are examined separately, the fiber diameter increases due to the increase in flow rate. On the other hand, when the fiber diameter measurements of Figure 8. B and D are examined, and no change is observed in the average fiber diameter despite the flow rate. So change in flow rate is compensated by voltage as voltage is 18kV in these groups compared to 22 kV in A and C. Finally, cracks were observed in the fibers in Figure 8. D. At low flow rates, the reduction in fiber diameter could not be tolerated by the voltage reduction, and cracks occurred 10 cm away. In the wet electrospinning method, the coagulation bath affects the fiber morphology. The coagulation bath must not be a solvent for the polymers (Mejía Suaza et al., 2022) . Although cellulose acetate is a polymer that is insoluble in water, fiber dissolution occurred in the collection fluid added with tween80 as seen in Figure 8. E and F.

CA nanofibers offer additional benefits for various applications, such as high surface area, high porosity, and lightweight, in addition to being biodegradable and biocompatible. The performance of CA nanofibers is directly influenced by their quality, which is defined by the fiber diameter, pore size, and fiber defect prevalence. The parameters of the electrospinning process, in turn, directly impact the quality of the fiber (Angel et al., 2020).

Core phase (PCL/Gel) electrospinning optimization studies were done with groups and conditions presented in Table 3.3.

Table 3.3 Experiment groups and parameters of PCL-Gel.

Sample	**Concentration**	**Parameters**	**Collector**	**Results**
PCL-Gel+HFIP	10% (80:20)	1 mL/h, 18 kV, 10 cm	Ethanol	Fiber obtained
PCL-Gel+HFIP	10% (80:20)	1 mL/h, 22 kV, 10 cm	Ethanol	Fiber obtained
PCL-Gel+HFIP	10% (80:20)	9 mL/h, 22 kV, 10 cm	Ethanol	No smooth fiber
PCL-Gel+HFIP	10% (80:20)	9 mL/h, 18 kV, 10 cm	Ethanol	No smooth fiber
PCL-Gel+HFIP	10% (80:20)	5 mL/h, 18 kV, 10 cm	Ethanol	Insufficient voltage value
PCL-Gel+HFIP	10% (80:20)	5 mL/h, 22 kV, 10 cm	Ethanol	Insufficient voltage value
PCL-Gel+HFIP	15% (1:1)	1 mL/h, 22 kV, 10 cm	Ethanol	Ribbon-shaped fibers

PCL-Gel+HFIP	15% (1:1)	0.5 mL/h, 22 kV, 10 cm	Ethanol	No homogeneous fiber
PCL-Gel+HFIP	15% (1:1)	0.7 mL/h, 18 kV, 10 cm	Ethanol	Fracture in fibers

As mentioned in the comparison of the fibers prepared with cellulose acetate solution, when Figure 9. A and B, C and D, and E and F are compared to each other, fiber diameters have decreased as the voltage increased. When Figure 9. C and D are compared to other flow rates (Figure 9. A, B, E, and F), it was not possible to obtain smooth fibers at a flow rate of 9 ml/h because the amount of solution was too high and the solvent did not evaporate completely. In addition, when Figure 9. C and D are examined, it is seen that the fiber morphology changes even with the high flow rate, and fibers begin to form under high voltage. In the same way, when Figure 9. E and F are examined, and it is seen that the solution and fiber appear together because the solution at a flow rate of 5 ml/h is not sufficiently electrified under low voltage. When the voltage is increased, the solution at the needle tip can be more electrified, so thicker fibers (thicker because the flow rate is increased) can be produced in Figure 9. F than in A and B. As mentioned above, ribbon-shaped fibers can be seen when the critical flow rate is exceeded. As the gelatin amount in the solution increases, a more fluid solution is obtained. In Figure 9. G, H, and I, 15% concentration and 1:1 ratio PCL-Gel solution were used. In Figure 9. G, ribbon-shaped fibers were produced because the flow rate exceeded the critical flow rate. When the flow rate is reduced, the fiber diameters decrease (Figure 9. H and I). In addition, when Figure 9. I am examined, beads are formed because the flow rate is increased and the voltage is reduced.

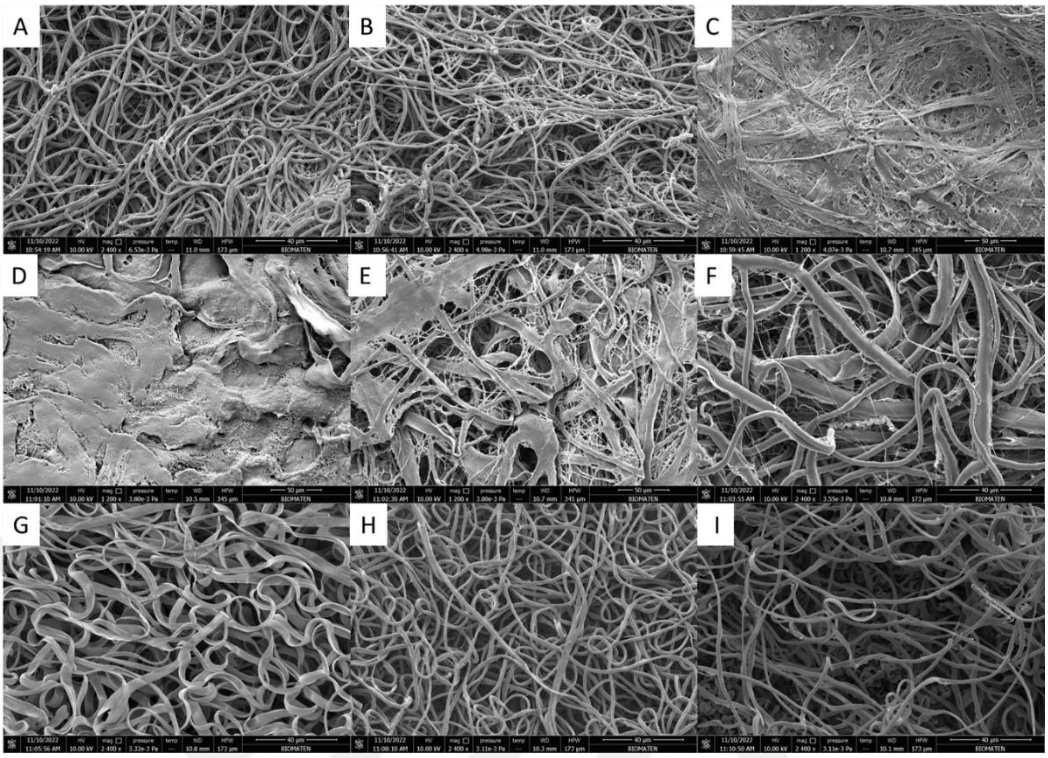

Figure 9. SEM images at 2400x of (A) PCL-Gel in ethanol (10% w,v (ratio 8:2), 18 kV, 1 mL/h, 10 cm), (B) PCL-Gel in ethanol (10% w,v (ratio 8:2), 22 kV, 1 mL/h, 10 cm), (C) PCL-Gel in ethanol (10% w,v (ratio 8:2), 22 kV, 9 mL/h, 10 cm), (D) PCL-Gel in ethanol (10% w,v (ratio 8:2), 18 kV, 9 mL/h, 10 cm), (E) PCL-Gel in ethanol (10% w,v (ratio 8:2), 18 kV, 5 mL/h, 10 cm), (F) PCL-Gel in ethanol (10% w,v (ratio 8:2), 22 kV, 5 mL/h, 10 cm), (G) PCL-Gel in ethanol (15% w,v (ratio 1:1), 22 kV, 1 mL/h, 10 cm), (H) PCL-Gel in ethanol (15% w,v (ratio 1:1), 22 kV, 0.5 mL/h, 10 cm), (I) PCL-Gel in ethanol (15% w,v (ratio 1:1), 18 kV, 0.7 mL/h, 10 cm).

Co-axial electrospinning experiments were performed with the parameters obtained from the results of these single electrospinning experiments. Optimization experiments were done and scaffolds with core/shell fiber structure were collected with the parameters shown in Table 3.4.

When the SEM images of the samples (Figure 10) were examined it was observed that core/shell fibers could not be produced at flow rates of 12 mL/h and above. A voltage value of 18 kV was also insufficient for fiber production. Since the 15% CA concentration was not fluid enough for co-axial electrospinning, optimization studies were carried out on the 12% CA concentration. Since fibers could not be collected at a 10 cm distance, the distance was reduced to 6 cm. When the co-axial electrospinning images were examined, the flow rate of 12 mL/h prevented the formation of cellulose acetate fibers. When Figure 10. (A) and (B) are examined, it is thought that the fibers formed are from the core solution, and a homogeneous core-shell structure could not be seen. When the flow rate of cellulose acetate was decreased, non-uniform and beaded fiber production occurred (Figure 10. (C)). Due to reducing the voltage from 22 kV to 18 kV, it could not create the electrical field that would allow cellulose acetate to form fibers at a flow rate of 5 ml/h. (Figure 10. (D)). As a result of these experiments, it was concluded that a flow rate of 5 is the critical level for cellulose acetate. The effect of distance and voltage is thought to be among the reasons for the image formed in Figure 10. D, fibers shown in Figure 10. E was produced by keeping the flow rate of 5 ml/h constant and changing the distance and voltage. According to SEM images, scaffold production parameters were selected as 8 cm distance, 22 kV voltage value, 1 mL/h flow rate of core polymers' solution (%10;80:20 w:w) w:v PCL-Gel) and 5 mL/h flow rate of shell polymer solution (%12 w:v CA)) which had the desired final core/Shell fiber structure in SEM Figure 10. E.

Table 3.4 Optimization groups and parameters for dual layer (core/shell) electrospinning experiments.

Sample Concentration	**Flow PCL-GEL**	**Flow CA**	**Voltage and distance**	**Collector**	**Results**
12% CA (w,v) 10% PCL-GEL (80:20 w,v)	1 mL/h	12 mL/h	22 kV, 6 cm	Ethanol	No fiber

12% CA (w,v) 10% PCL-GEL (80:20 w,v)	1 mL/h	12 mL/h	18 kV, 6 cm	Ethanol	No fiber
12% CA (w,v) 10% PCL-GEL (80:20 w,v)	1 mL/h	9 mL/h	22 kV, 6 cm	Ethanol	Solvent evaporation insufficent
12% CA (w,v) 10% PCL-GEL (80:20 w,v)	1 mL/h	5 mL/h	18 kV, 6 cm	Ethanol	Insufficient voltage value
12% CA (w,v) 10% PCL-GEL (80:20 w,v)	1 mL/h	5 mL/h	22 kV, 8 cm	Ethanol	Good and homogeneous fibers

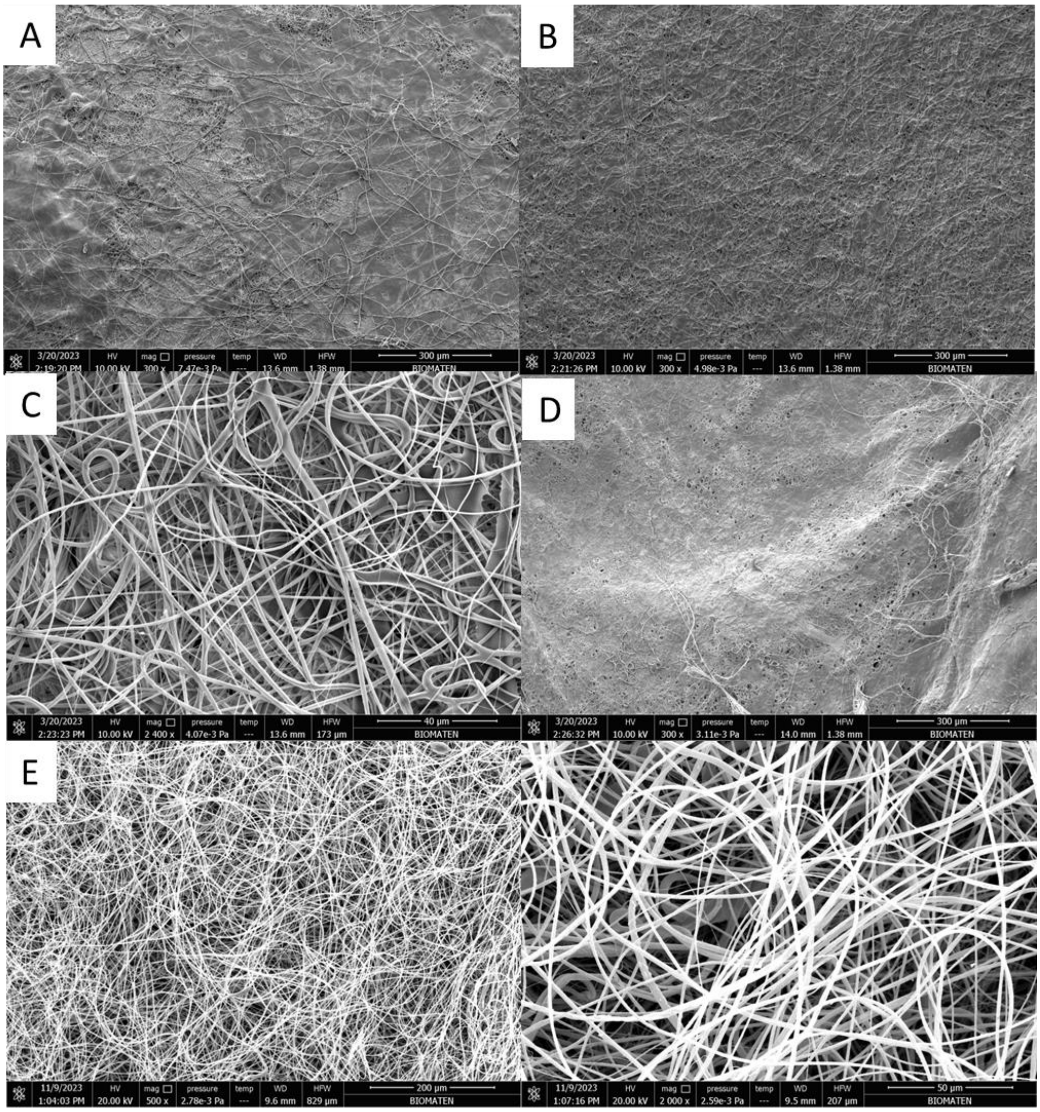

Figure 10. SEM images of core shell scaffold produced in optimization studies: A) PG/C 1 12% CA (w,v)/10% PCL-GEL (80:20 w,v) in ethanol (22 kV, 12/1 mL/h, 6 cm, 300x), B) 12% CA (w,v)/10% PCL-GEL (80:20 w,v) in ethanol (18 kV, 12/1 mL/h, 6 cm, 300x)PG/C 2, PG/C 3 (C) 12% CA (w,v)/10% PCL-GEL (80:20 w,v) in ethanol (22 kV, 9/1 mL/h, 6 cm, 2400x), PG/C 4 (D) 12% CA (w,v)/10% PCL-GEL (80:20 w,v) in ethanol (18 kV, 5/1 mL/h, 6 cm, 300x), (E) 12% CA (w,v)/10% PCL-GEL (80:20 w,v) in ethanol (22 kV, 5/1 mL/h, 8 cm. at 500x and 2000 x).

3.1.3 In vitro Water Uptake and Degradation of Scaffolds

Synthetic polymers and composites of synthetic polymers with natural polymers are widely used in controlled drug delivery and tissue engineering applications due to their improved degradation rates. The degradation rate is important for cellular activities such as cell proliferation, tissue regeneration, and host response (Sung et al., 2004).

As a result of the 14-day degradation experiments, the dry weights of the samples were not changed (Figure 11 (A)). However, when the degradation SEM images of the samples were examined (Figure 12), it was observed that deformations and small degenerations indicated that degradation in the form of surface erosion had started on fibrous structures of scaffolds.

The water retention percentage of the scaffold is important for cell distribution, nutrient, and waste transfer (Sung et al., 2004). In the experiment, it exceeded 1200%. It is thought that gelatin increases the water retention capacity due to its hydrophilic structure.

In a study by Nosar et al., cellulose acetate showed significant degradation in vitro after 30 days (Nosar et al., 2016). In another study by Sung et al., PCL was found to undergo a significant 39% degradation in vitro in 28 days (Sung et al., 2004).

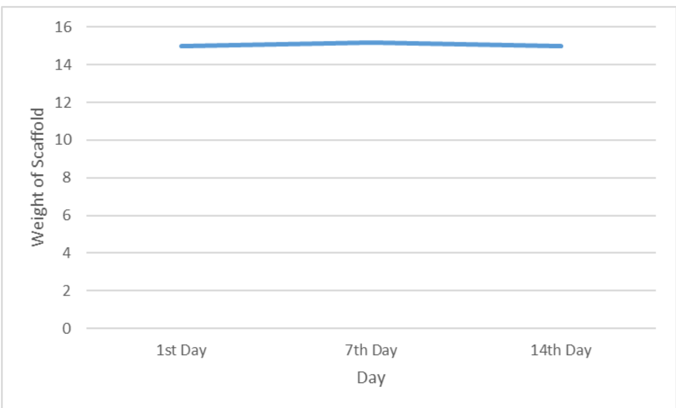

Figure 11. Degradation (A) result of PCL-Gel/Ca (10% (8:2),12%, 22 kV, 1/5 mL/h, 8cm) for 14 days in PBS.

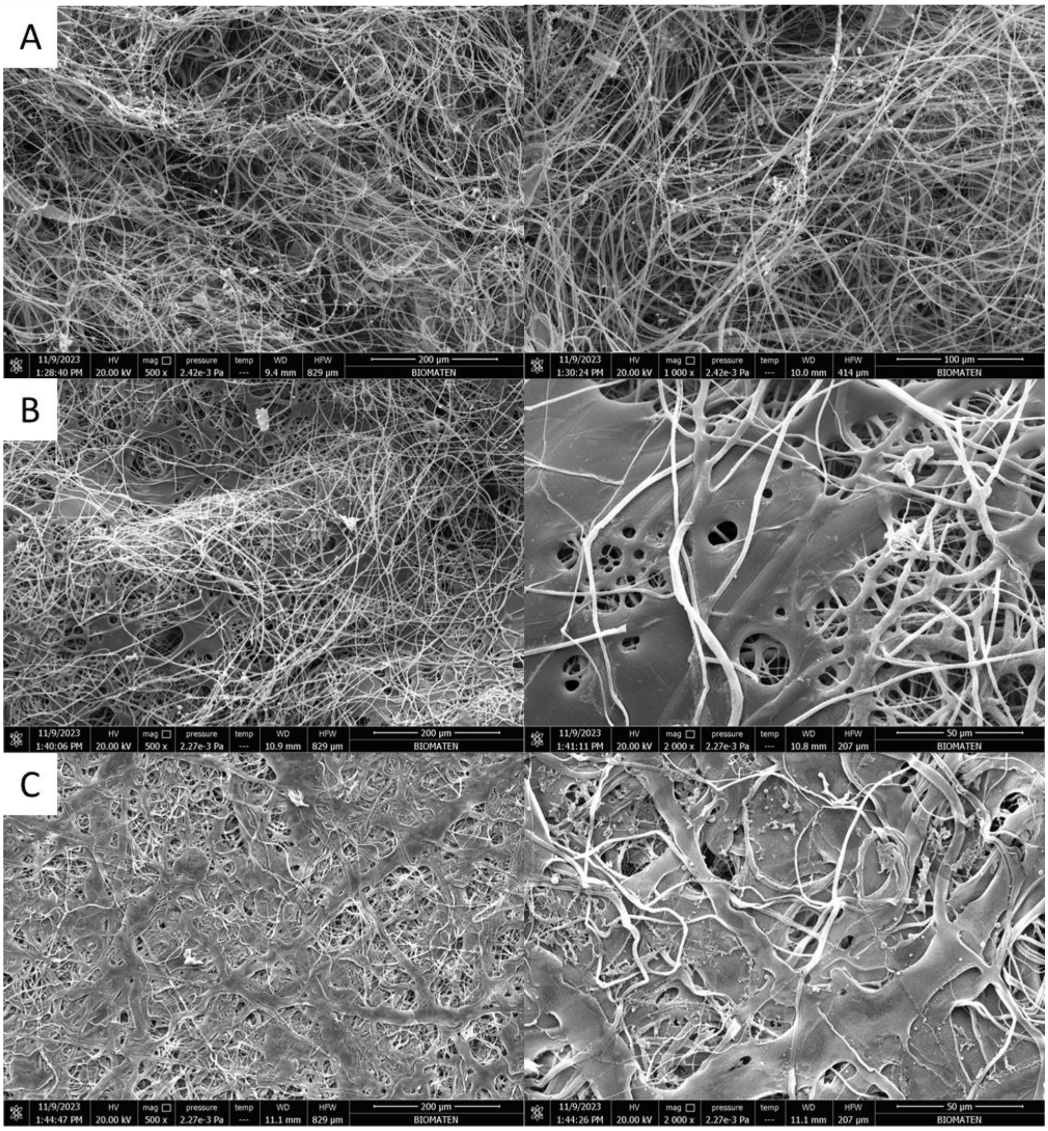

Figure 12. SEM degredation images at 500 and 2000 x of PCL-Gel/Ca (10% (8:2),12%, 22 kV, 1/5 mL/h, 8cm) for 14 days. (A) 1st day, (B) 7th day, (C) 14th day.

3.1.4 Protein/Peptide Release Results of Scaffolds

In drug delivery studies, electrospinning methods are one of the preferred ways for developing drug delivery systems that can be designed according to the release rate requirements; immediate release, sustained release, and continuous release (Yan et al., 2014). Drug release can occur immediately with the bursting effect as a result of loading the drug on/close to the surface of fibers, or the drug can be released in a controlled and longer period by eliminating the immediate release effect with the core-shell method in which drug that will be released is loaded in the core and covered with an outer shell barrier (Yan et al., 2014). In a study by Yu et al., the release of the drug spun with cellulose acetate loaded separately on the shell and core were compared. The same drug (Ferulic acid) was loaded separately into both the shell and the core. While the drug loaded in the shell region was released immediately, the drug loaded in the core was released for a longer period without being affected by the immediate release effect (Yu et al., 2013). In another study, researchers developed a drug delivery system produced by the coaxial electrospinning method with a shell of PCL, and core from Gel with a lawsone (hennotannic acid). Thereby, reducing the immediate release effect of the drug and releasing it for a longer period was achieved (Adeli-Sardou et al., 2019).

In this thesis, HIF1-α alpha was loaded on the shell because its immediate release was desired. On the other hand, the ghrelin molecule was loaded in the core of the scaffold for a longer period of controlled release. As seen in release studies (Figure 13 (A)) of single protein/peptide loaded core/shell fibrous scaffolds, the HIF1-α protein in the shell part of the scaffold made of CA has been released immediately. The ghrelin peptide which is loaded in PCL-Gel (the core of the scaffolds) to support both osteogenesis and angiogenesis has shown less immediate release effect and its controlled and extended release profile was achieved (Figure 13 (B).

To the thesis goal, the HIF1 ɑ protein was loaded onto the shell of the double-layered scaffold. According to the release results of this scaffold (Figure 13) there was a burst release on 1st day which continued with a slower release profile on the 2nd day. The release of HIF1- ɑ was much slower for the following days. This fast-release profile was expected as the loaded molecules were at the shell of the fibers of the scaffold and HIF1 ɑ is a water-soluble protein. The ghrelin peptide, which was loaded into the core of the double-layered scaffold was expected to show a slower release over a longer period. This was seen in the ghrelin release profile which was in a controlled and prolonged manner, thus providing an extended release duration continuouing throgh 10 days.

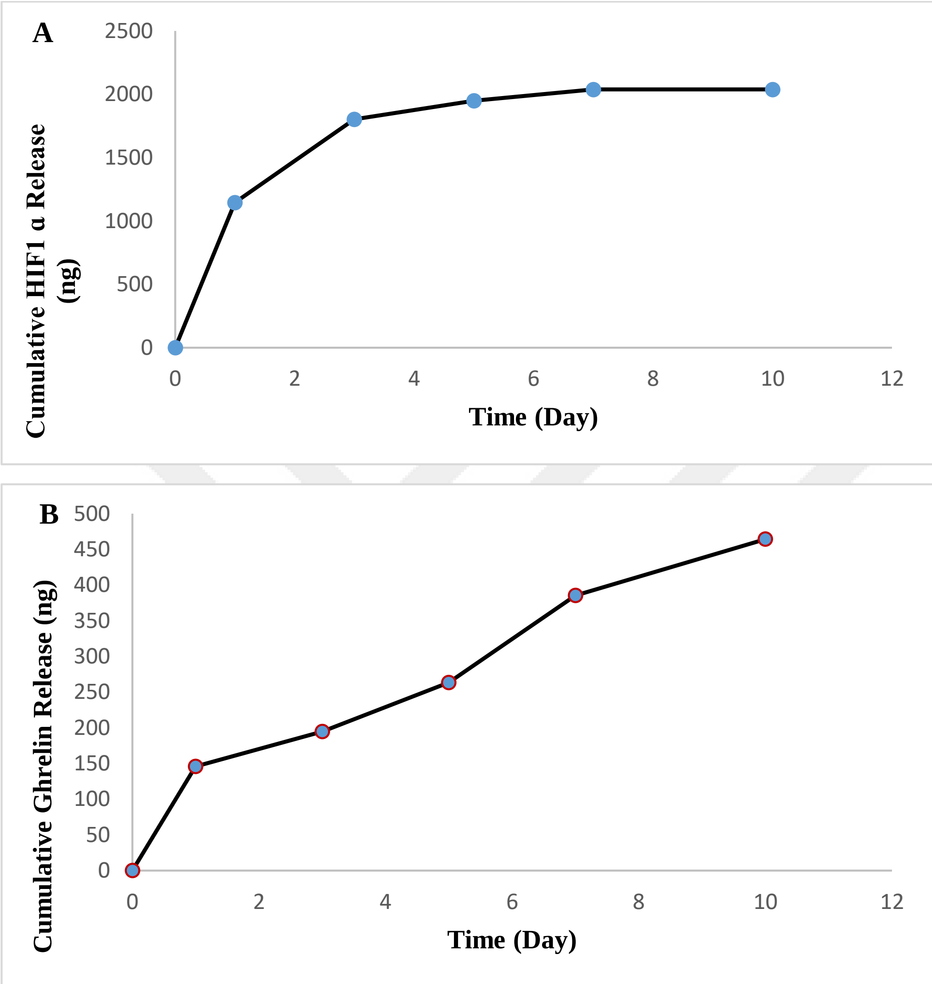

Figure 13. Cumulative HIF1 α release (A), cumulative Ghrelin release (B) for 10 days in PBS (pH 7.4, 0.01 M).

3.1.5 Cell Attachment Properties of Scaffold

The adhesion and proliferation of cells (HUVEC and HFOB) to the produced scaffold and protein-loaded scaffolds (scaffold loaded with HIF1 α and scaffold loaded with ghrelin) were investigated by taking SEM images on 1st, 3rd, and 7th day (Figure 14 and 15). It was observed that both cell types adhered to the scaffolds at the end of day 1 (Figure 14. (A), (D) and 15. (G), (J)). By the end of day 3, it was observed that the cells were gradually proliferating on the scaffolds (Figure 14. (B), (E) and (H), (K)). By the end of day 7, they had covered some parts on the surface of the scaffolds (Figure 14. (C), (F) and (I), (L)). In conclusion, the scaffolds (loaded and unloaded with protein) adhered to both cell types and provided a suitable environment for their growth over time.

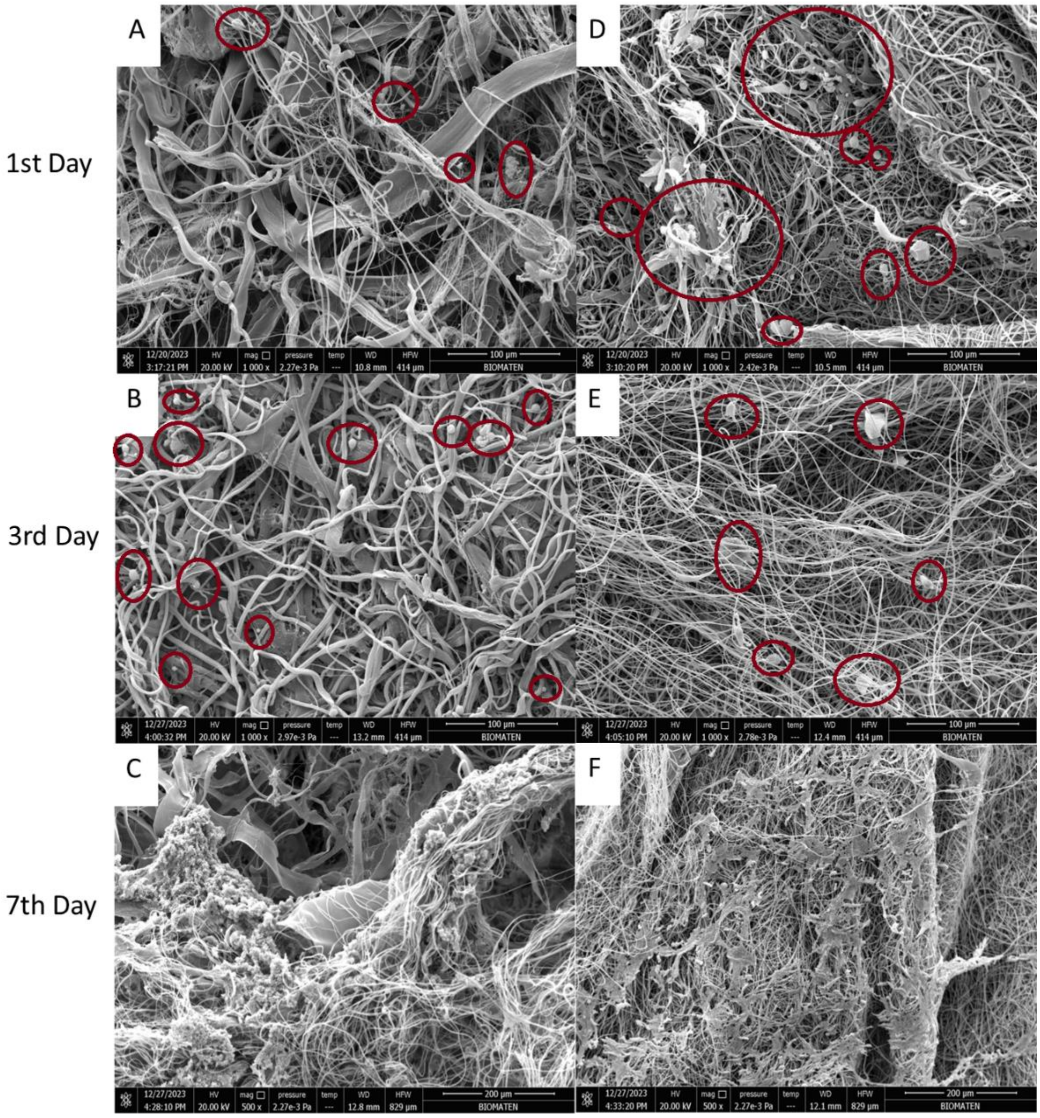

Figure 14. SEM images showing HUVEC cell attachment on the scaffolds. Scaffold (w/o ghrelin and HIF1-ɑ with HUVEC cell 1st day (A), Scaffold (w/o ghrelin and HIF1-ɑ) with Huvec cell 3rd day (B), Scaffold (w/o ghrelin and HIF1-ɑ) with Huvec cell 7th day (C), Scaffold (w/o ghrelin, with HIF1-ɑ in shell) with Huvec cell 1st day (D), Scaffold (w/o ghrelin, with HIF1-ɑ in shell) with Huvec cell 3rd day (E), Scaffold (w/o ghrelin, with HIF1-ɑ in shell) with Huvec cell 7th day (F)

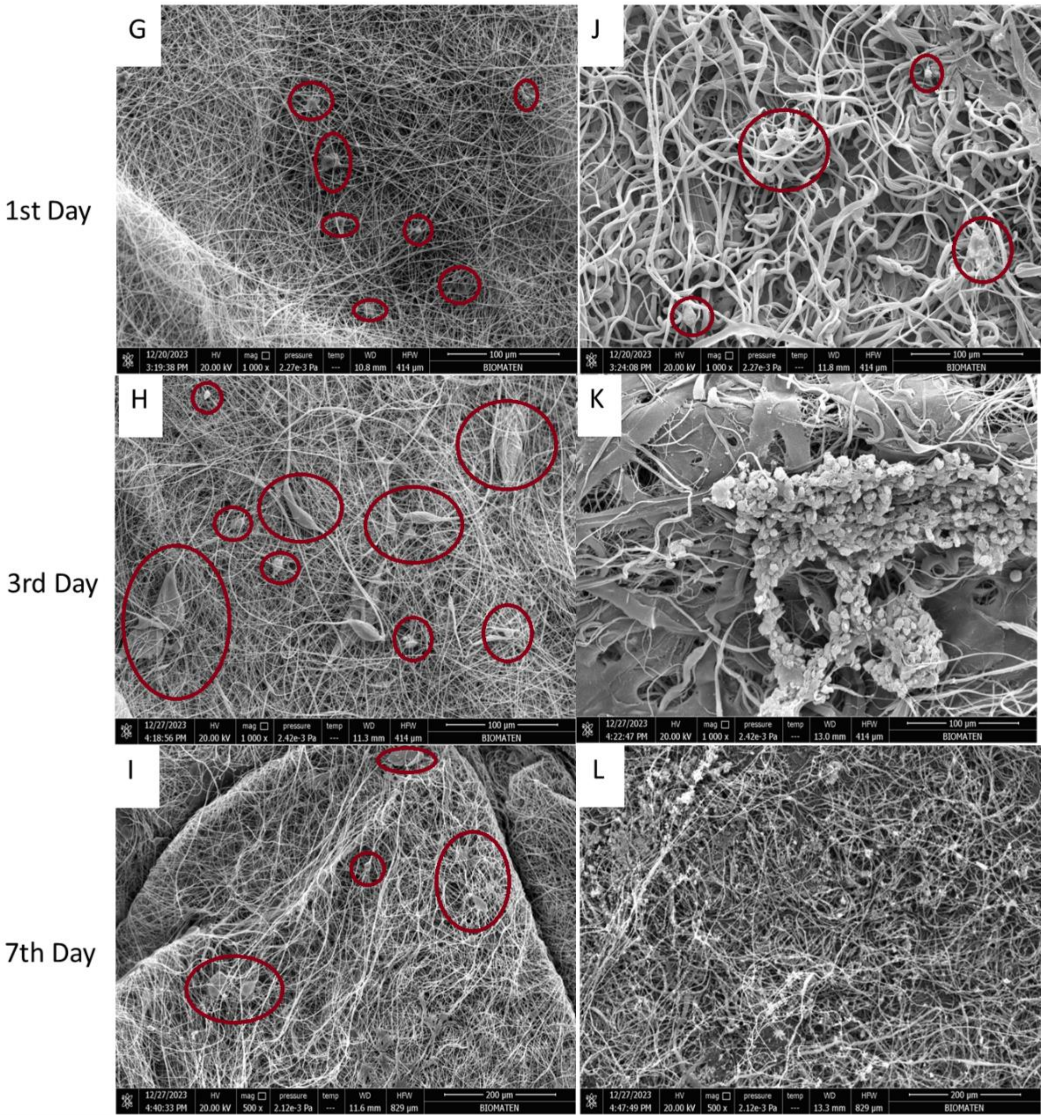

Figure 15. SEM images showing HFOB cell attachment on the scaffolds. Scaffold (with ghrelin in the core, w/o HIF1-ɑ) with HFOB cell 1st day (G), Scaffold (with ghrelin in the core, w/o HIF1-ɑ) with HFOB cell 3rd day (H), Scaffold (with ghrelin in the core, w/o HIF1-ɑ) with HFOB cell 7th day (I), Scaffold (w/o ghrelin and HIF1-ɑ) with HFOB cell 1st day (J), Scaffold (w/o ghrelin and HIF1-ɑ) with HFOB cell 3rd day (K), Scaffold (w/o ghrelin and HIF1 ɑ) with HFOB cell 7th day (L).

3.2 Cell Culture Experiments

3.2.1 Dose Studies

3.2.1.1 HIF1-α

Literature studies on HIF1-α have generally examined the increase in HIF1-α levels in response to hypoxic conditions, depending on the amount of VEGF. When the study conducted by Xie et al. was examined, it was seen that the HIF1-α level in the cells was 2 ng for the minimum amount of VEGF required to initiate angiogenesis (Xie et al., 2014). Therefore, it was decided to study the dose range 2-8 ng for in vitro experiments. To determine the effective dose of HIF1-α, 10,000 HUVEC cells were exposed to different amounts of HIF1-α on the first day. The effect of HIF1 α on HUVEC cells was examined for 7 days. As seen in the cell viability assay results (Figure 16. A), HIF1 α was found to increase cell viability after 24 and 48 hours of exposure. In addition, to find the effective dose amount that increases the amount of VEGF in HUVEC cells, VEGF amount measurements were performed with the ELISA kit after 24 and 48 hours of exposure to HIF1-α. As a result of these measurements, all doses showed a significant increase in VEGF production amount compared to the control group ($p<0,001$) after 24 h HIF1-α and 48 h HIF1-α exposion (Figüre 16. (B)). However, with the insight to give the body the smallest amount of a foreign and potential protein, a 2 ng dose of HIF1-α protein was selected as the effective dose and considered as the target dose in further experiments.

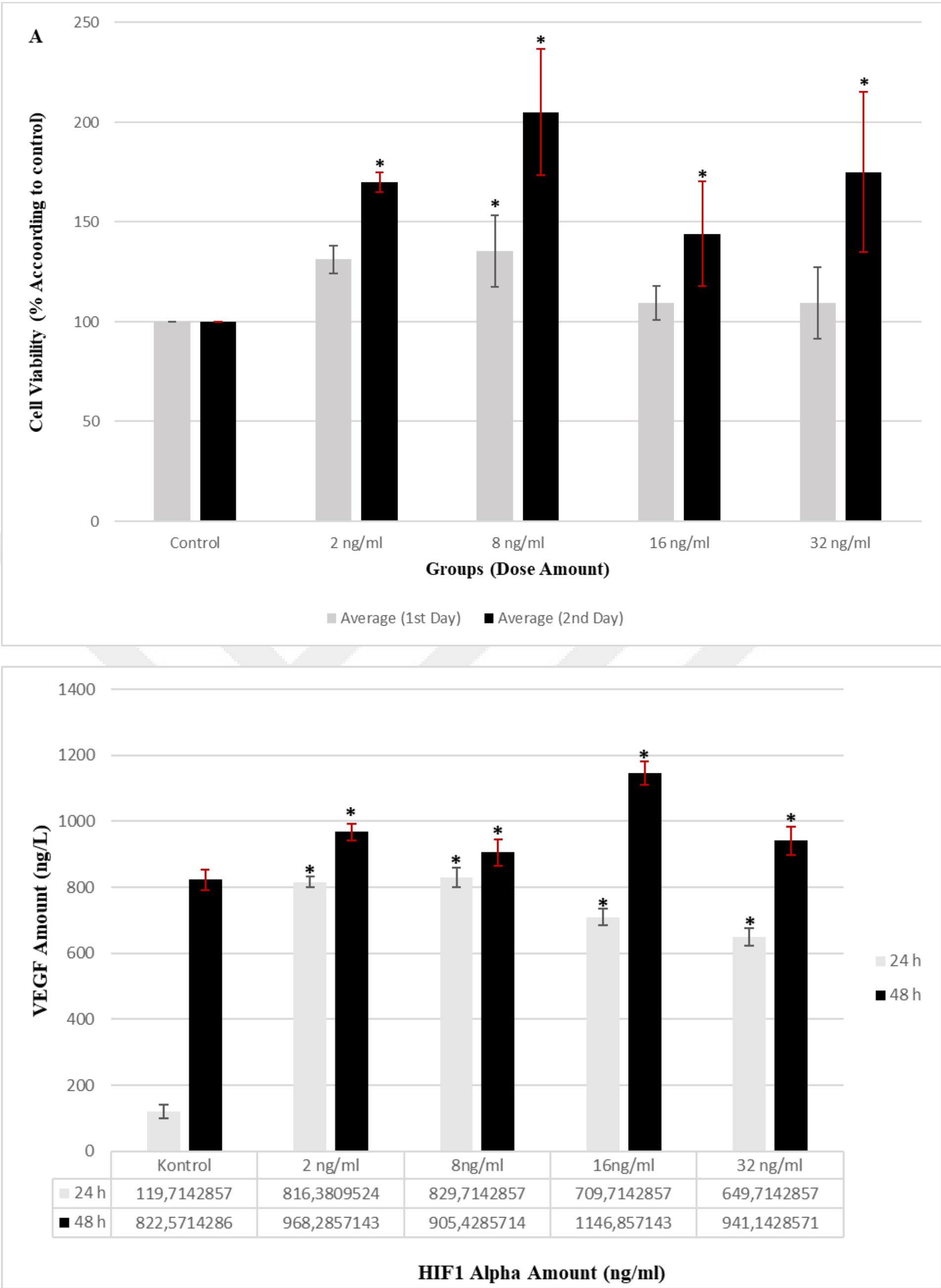

Figure 16. Cell culture experiments with HUVEC cells exposed to different doses of HIF1-α. A) Analysis of Cell Viability in Cells Treated with Different Doses of HIF1 α, B) Average amounts of VEGF produced by cells exposed to different amounts of HIF1-α. Control group; HUVEC Cells. * denote statistically significant results with p<0.01 according to control.

3.2.1.2 Ghrelin

A literature review found that ghrelin was studied in the dose range of 1-10 nM (Li et al., 2007). Therefore, to determine the effective ghrelin dose, 10 000 HFOB cells were seeded and incubated for 24 hours at 37 ℃ in media containing different amounts of ghrelin (5, 10, 20, 40 nM). After 24 hours of ghrelin exposure, cell media changed with ghrelin-free media. Cell viability measurements were performed 24 and 72 hours after ghrelin exposure. After 24 hours of ghrelin exposure, the cell culture experiment continued with ghrelin-free HFOB media. As seen in Figure 17. (A), when the viability percentages were calculated relative to the control group, no improvement effect of ghrelin on viability was observed at different doses; 5,10, 20, and 40 nM.

As early osteogenic differentiation marker ALP (alkaline phosphatase enzyme activity of osteoblast cells was measured after exposing cells to the above doses of ghrelin.

In the dose experiment, there were observed significantly differences in the ALP results of cells exposed to 5 nM and 20 nM ($p<0,05$) ghrelin on the 14th day compared to control cells (Figure 17. (B)). Although the ALP results of the 20 nM ghrelin group were also good, this group was not chosen due to its slightly lower cell viability results. Considering the ALP results and cell viability results, 5 nM was chosen as the effective dose.

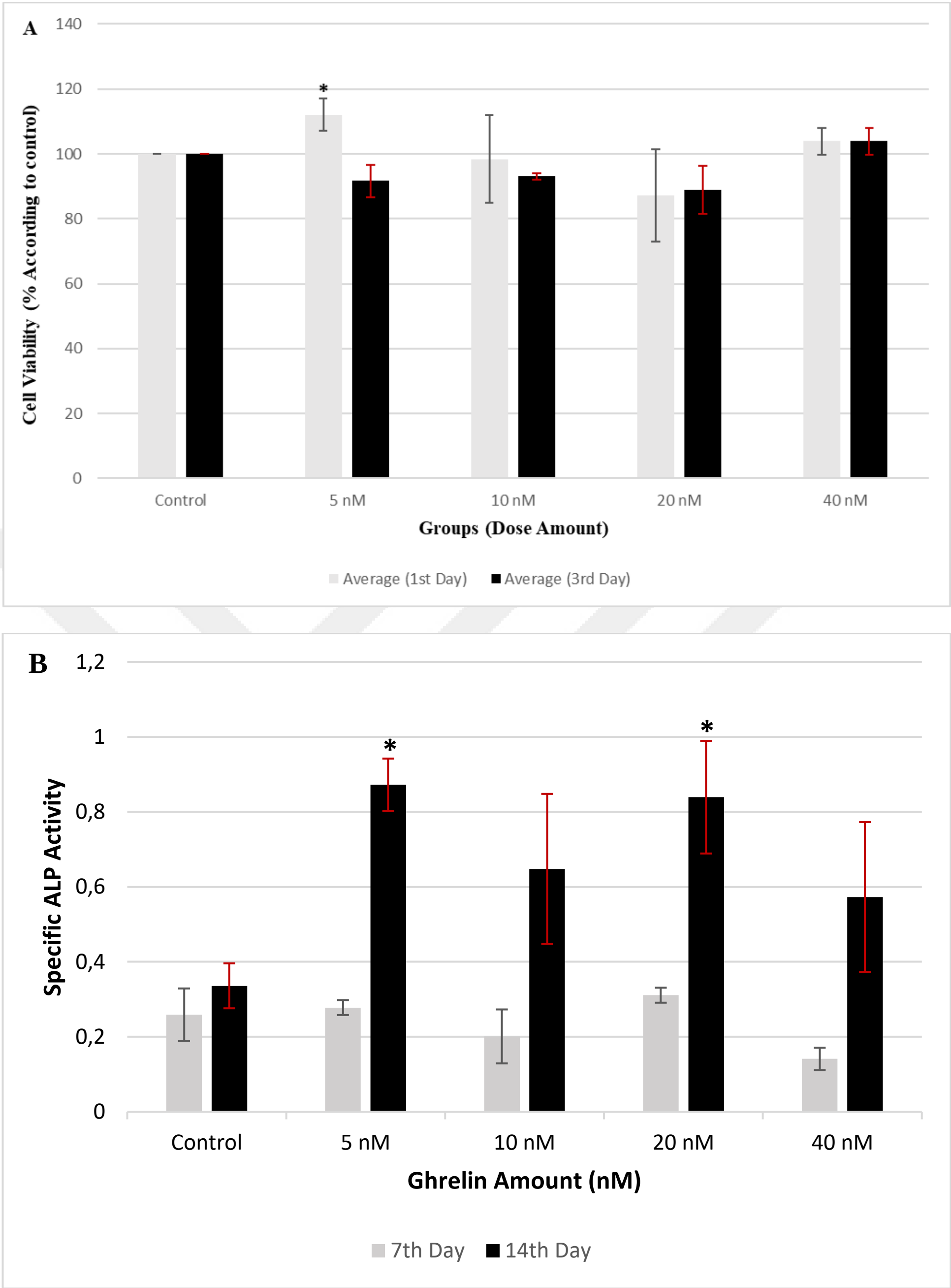

Figure 17. Cell culture experiments with HFOB cells exposed to different doses of Ghrelin A) Ghrelin doses effect on cell viability), B) Ghrelin effect on ALP result after 7th and 14th days (with 5,10,20 and 40 nM). * denote statistically significant results with $p<0.05$ according to control. (Control group: HFOB cells with growth media.)

3.2.2 HIF1-α/Ghrelin Loaded Scaffolds

Scaffolds loaded with HIF1-α or Ghrelin and without any protein/peptide loading were grouped as shown in Table 3.5.

For evaluation of the biological activity of HIF1-α loaded scaffolds; scaffolds loaded with HIF1-α, w/o ghrelin and scaffold without any protein were prepared and incubated in 250 µl of cell culture media for 24 hours, and then the media was transferred to cell culture plates of HUVEC cells that were incubated at 37°C for 24 hours. The cells that were exposed to the media (in which the scaffold was incubated for 24 hours) were evaluated for cell viability at days 1, 3, and 7, and the amounts of VEGF that the cells released were measured at the same time points. As shown in Figure 18. (A), there was a slight decrease in cell viabiliteis in the 1st day, but the cell viability results after the third day was similar with was no significant differance among groups and with control.

When, the VEGF levels taken at three different times (1st, 3rd and 7th days) were examined (Figure 18 B), significant increase in the VEGF levels of the cells exposed to HIF1-α was observed compared to the control cells ($p<0.01$).

In the literature, many studies have been conducted to investigate the effects of the HIF1-α molecule on angiogenesis. In a study by Chen Li and colleagues, they investigated the function of HIF-1 α in angiogenesis in the region of bone defect under normoxic (normal oxygen level in the blood) conditions. It was observed that HIF1-α significantly increased VEGF production and also supported osteogenesis (C. Li et al., 2013). Jingyi Li and colleagues placed hydroxyapatite scaffolds seeded with mesenchymal stem cells stimulated with 3A and HIF-1 α in the calvarial defect region of mice and investigated the effects of HIF1-α and SEMA3A on angiogenesis and osteogenesis. By the end of eight weeks, there was a significant increase in the expression of genes involved in the osteogenic and angiogenic processes (J. Li et al., 2020).

For evaluation of the biological activity of scaffolds (w/o ghrelin and loaded with HIF1-ɑ)), and scaffolds (loaded with ghrelin) (Table 3.5) were incubated in 250 µl volume of media at 37°C for one day, and then the media was transferred to wells containing HFOB cells. Cell viability was evaluated at 1 and 3 days after transfer. As shown in Figure 19. (A), ghrelin had a positive effect on cell viability ($p<0.01$).

Osteogenic differentiation analysis was performed by ALP assay on the same samples at 7 and 14 days after transfer.

As seen in Figure 19. (B), although ALP activities of scaffolda and control were comaprable at fay 7, there was a consideravle (about 2.5 fold) incresase in ALP activity for ghrelin loaded scaffolds compared to control and only scaffold group. ($p<0.01$). Research on the ghrelin hormone has shown that ghrelin, a 28-amino acid hunger-stimulating peptide hormone produced in the stomach fundus and pancreas, supports angiogenesis and osteogenesis. In a study conducted by a research group, the effect of ghrelin on the healing of femur shaft fractures was investigated. According to the results obtained after ghrelin was injected daily into mice, it was shown that it directly contributes to fracture healing (Erener et al., 2021). Yuan et al., on the other hand, injected ghrelin to the experimental group and saline to the control group for 4 weeks to investigate the effect of ghrelin on angiogenesis in a myocardial infarction mouse model. In the results, higher alpha-SMA positive vessel formation was observed in the group treated with ghrelin, and a significant increase was observed in the expression of VEGF in the infarction region (Yuan et al., 2012).

Table 3.5 Groups of scaffolds for cell culture experiments

Scaffold	**Core**	**Shell**	**Protein amount**
PCL-Gel/CA	-	-	-
PCL-Gel/CA	-	HIF1 α	5000 ng
PCL-Gel/CA	Ghrelin	-	5000 ng

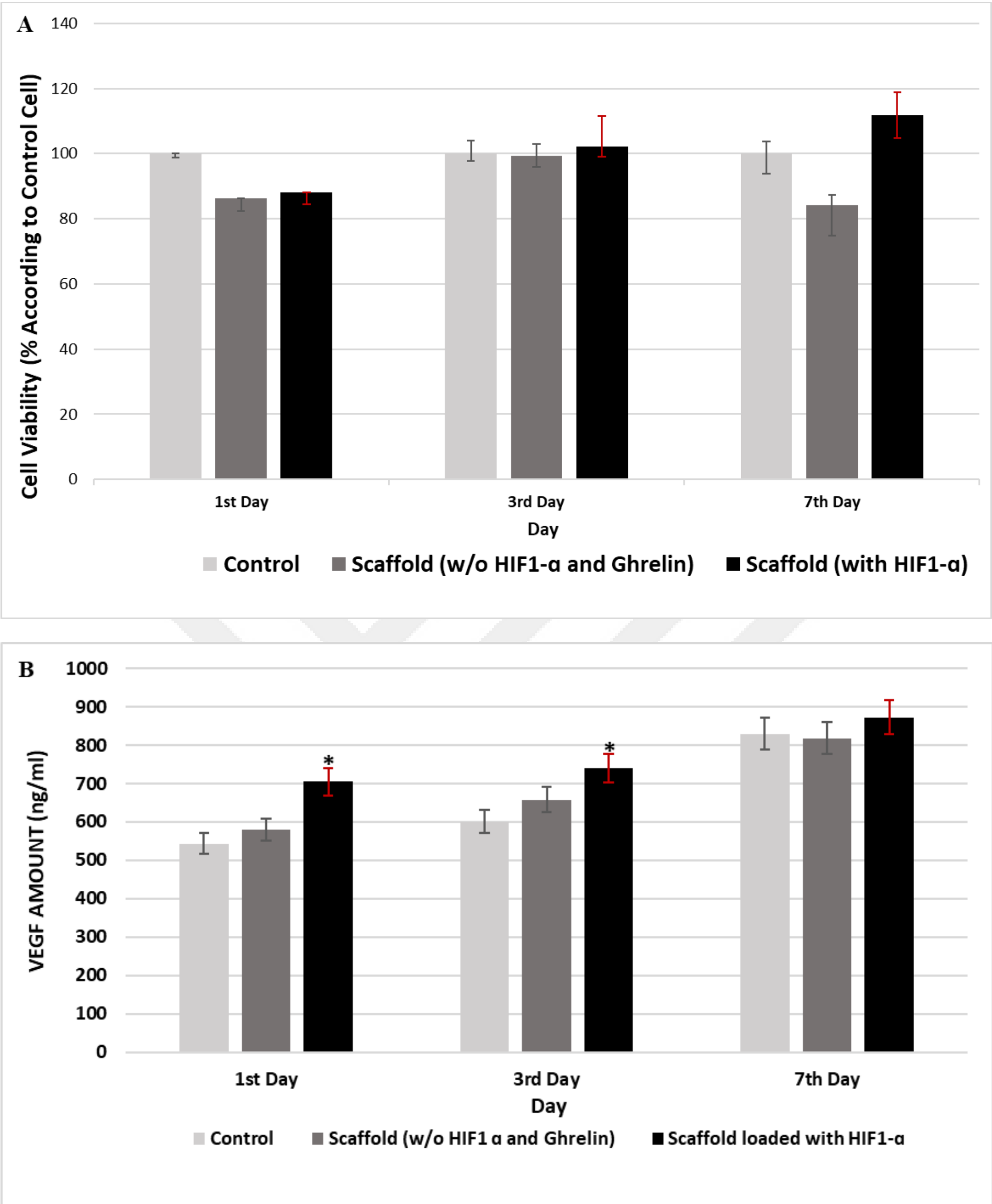

Figure 18. (A) Cell viability (%) for 7 days result of HIF1 α (n=3). (B) VEGF amounts of Scaffold Loaded HIF1-α and empty scaffolds HIF1-α (n=3). * denote statistically significant results with p<0.01 according to control.

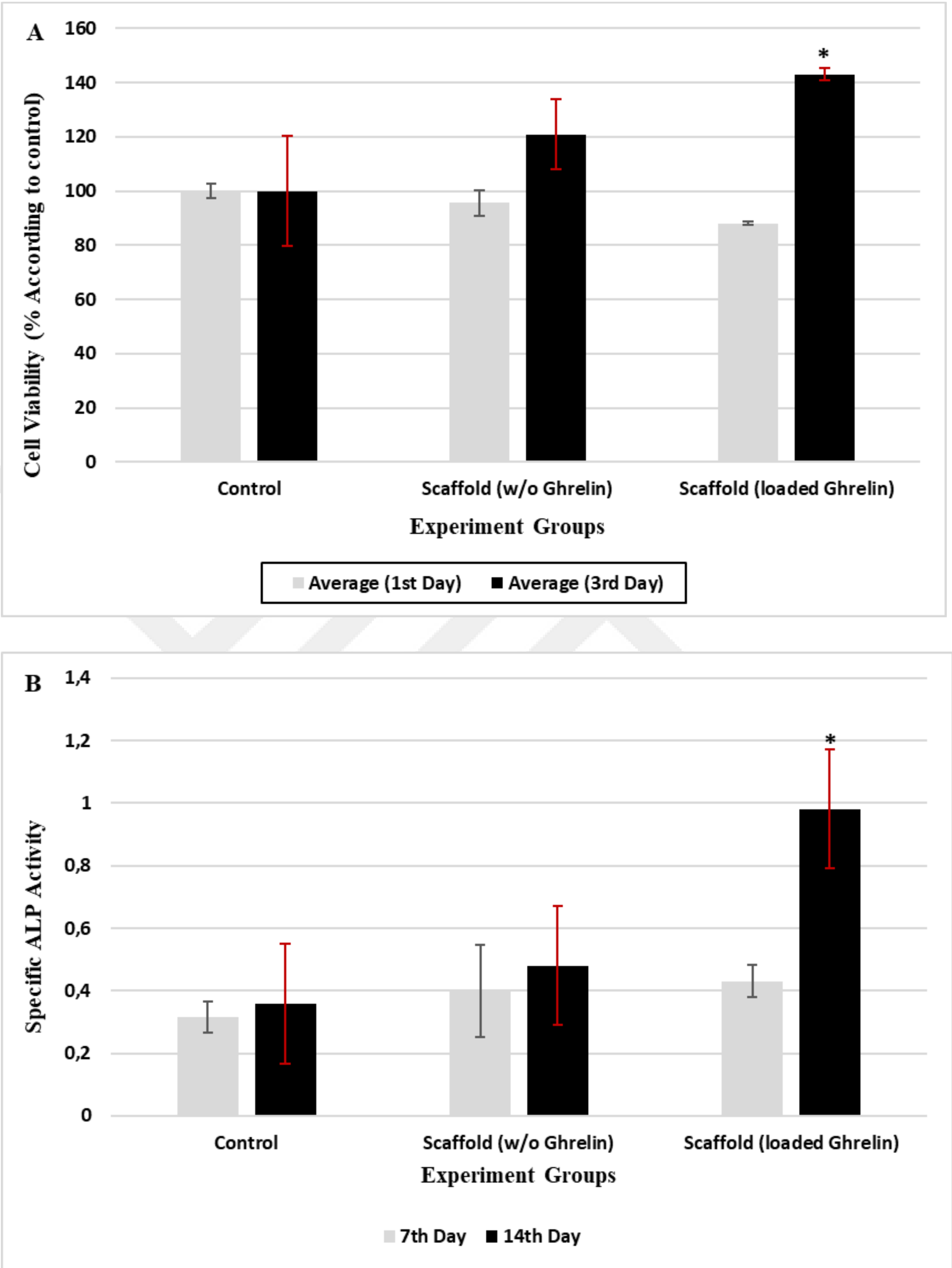

Figure 19. (A) Cell viability (%) for 3 days of Ghrelin administration (n=3). (B) ALP result for 7 and 14 days after Ghrelin loaded or empty scaffold administration (n=3). * denote statistically significant results with $p<0.05$ according to control.

CHAPTER 4

CONCLUSION

Co-axial electrospinning is a simple and widely used scaffold production method in tissue engineering. This method enables the production of scaffolds from double-layered fibers that allow the loading of different polymer compositions in the outer and inner layer of fibers besides loading different bioactive agents/molecules to different parts of fibers. This approach can also provide control of release profiles in dual molecule loaded scaffolds, In this thesis, 3D double-layered scaffolds were successfully produced by wet co-axial electrospinning with cellulose acetate (CA) shell layer and poly-caprolactone (PCL)/gelatin (Gel) polymers core layer of the fibers forming the scaffold. The rapid release of HIF-1 α protein which was loaded to the outer (Shell) polymer was achieved as initially aimed in the study for induction of angiogenesis for early start of vascularization at the defect site. In vitro studies supported the increase in VEGF production in HUVEC cells. The release of HIF1 α alpha protein from a carrier to stimulate VEGF production with the ultimate aim of overcoming the problem of insufficient vascularization, which is one of the limitations of bone tissue engineering, has not been tried before in the literature. The ghrelin peptide, known as the hunger hormone, had more slower release owing to its being loaded in the inner (core) component of the fibers. This was also to have a prolonged effect on this peptide as it is known to stimulate bone regeneration in literature. In vitro studies with ghrelin doses were also done for the first time in literature with HFOB cells. Besides that ghrelin loading and release were also not examined in another study. Ghrelin release from scaffolds was shown to have a positive effect on ALP activity on the 14th day. The dual release of HIF1 α and ghrelin hormone together from the same scaffold has also not been studied in the literature. This will be the continuation of this research in future studies. This study focused on the dual loading and release of a newly optimized coaxial electrospun scaffold for generating a bone tissue engineering scaffold that will improve both osteogenic activity and vascularization when used in vivo. For the thesis duration therefore it was not possible to add components like a bioceramic which is mainly used in BTE scaffolds for its importance in improving mechanical and the properties of scaffolds for bone regeneration. This concept is the limitation of this study.

REFERENCES

Abdullah, M. F., Andriyana, A., Muhamad, F., & Ang, B. C. (2023). Fabrication of poly(lactic acid)-cellulose acetate core-shell electrospun fibers with improved tensile strength and biocompatibility for bone tissue engineering. Journal of Polymer Research, 30(7), 1–16. https://doi.org/10.1007/S10965-023-03639-0/FIGURES/10

Adeli-Sardou, M., Yaghoobi, M. M., Torkzadeh-Mahani, M., & Dodel, M. (2019). Controlled release of lawsone from polycaprolactone/gelatin electrospun nanofibers for skin tissue regeneration. International Journal of Biological Macromolecules, 124, 478–491. https://doi.org/10.1016/J.IJBIOMAC.2018.11.237

Afewerki, S., Sheikhi, A., Kannan, S., Ahadian, S., & Khademhosseini, A. (2019). Gelatin-polysaccharide composite scaffolds for 3D cell culture and tissue engineering: Towards natural therapeutics. Bioengineering & Translational Medicine, 4(1), 96. https://doi.org/10.1002/BTM2.10124

Alipal, J., Mohd Pu'ad, N. A. S., Lee, T. C., Nayan, N. H. M., Sahari, N., Basri, H., Idris, M. I., & Abdullah, H. Z. (2021). A review of gelatin: Properties, sources, process, applications, and commercialization. Materials Today: Proceedings, 42, 240–250. https://doi.org/10.1016/J.MATPR.2020.12.922

Amini, A. R., Laurencin, C. T., & Nukavarapu, S. P. (2012). Bone Tissue Engineering: Recent Advances and Challenges. Critical Reviews in Biomedical Engineering, 40(5), 363. https://doi.org/10.1615/CRITREVBIOMEDENG.V40.I5.10

Amini, A. R., Laurencin, C. T., & Nukavarapu, S. P. (2012). Bone Tissue Engineering: Recent Advances and Challenges. Critical Reviews in Biomedical Engineering, 40(5), 363. https://doi.org/10.1615/CRITREVBIOMEDENG.V40.I5.10

Angel, N., Guo, L., Yan, F., Wang, H., & Kong, L. (2020). Effect of processing parameters on the electrospinning of cellulose acetate studied by response surface methodology. Journal of Agriculture and Food Research, 2, 100015. https://doi.org/10.1016/J.JAFR.2019.100015

Bahney, C. S., Zondervan, R. L., Allison, P., Theologis, A., Ashley, J. W., Ahn, J., Miclau, T., Marcucio, R. S., & Hankenson, K. D. (2019). Cellular biology of fracture healing. Journal of Orthopaedic Research : Official Publication of the Orthopaedic Research Society, 37(1), 35–50. https://doi.org/10.1002/JOR.24170

Baker, M. I., Walsh, S. P., Schwartz, Z., & Boyan, B. D. (2012a). A review of polyvinyl alcohol and its uses in cartilage and orthopedic applications. Journal of Biomedical Materials Research. Part B, Applied Biomaterials, 100(5), 1451–1457. https://doi.org/10.1002/JBM.B.32694

Baker, M. I., Walsh, S. P., Schwartz, Z., & Boyan, B. D. (2012b). A review of polyvinyl alcohol and its uses in cartilage and orthopedic applications. Journal of Biomedical Materials Research Part B: Applied Biomaterials, 100B(5), 1451–1457. https://doi.org/10.1002/JBM.B.32694

Barre, R., Beton, N., Batut, A., Accabled, F., Sales de Gauzy, J., Auriol, F., Eddiry, S., Tauber, M., Laurencin, S., Salles, J. P., & Gennero, I. (2020). Ghrelin uses the GHS-R1a/Gi/cAMP pathway and induces differentiation only in mature osteoblasts. This ghrelin pathway is impaired in AIS patients. Biochemistry and Biophysics Reports, 24, 100782. https://doi.org/10.1016/J.BBREP.2020.100782

Baumgarten, P. K. (1971). Electrostatic spinning of acrylic microfibers. Journal of Colloid and Interface Science, 36(1), 71–79. https://doi.org/10.1016/0021-9797(71)90241-4

Benoit, D. S. W., Schwartz, M. P., Durney, A. R., & Anseth, K. S. (2008). Small functional groups for controlled differentiation of hydrogel-encapsulated human mesenchymal stem cells. Nature Materials 2008 7:10, 7(10), 816–823. https://doi.org/10.1038/nmat2269

Bezwada, R. S., Jamiolkowski, D. D., Lee, I. Y., Agarwal, V., Persivale, J., Trenka-Benthin, S., Erneta, M., Suryadevara, J., Yang, A., & Liu, S. (1995). Monocryl® suture, a new ultra-pliable absorbable monofilament suture. Biomaterials, 16(15), 1141–1148. https://doi.org/10.1016/0142-9612(95)93577-Z

Biga, L. M., Bronson, S., Dawson, S., Harwell, A., Hopkins, R., Kaufmann, J., LeMaster, M., Matern, P., Morrison-Graham, K., Oja, K., Quick, D., Runyeon, J., OERU, O., & OpenStax. (2019). 6.2 Bone Classification. OpenStax/Oregon State University.

Carmeliet, P., & Jain, R. K. (2000). Angiogenesis in cancer and other diseases. Nature 2000 407:6801, 407(6801), 249–257. https://doi.org/10.1038/35025220

Claes, L. E., Heigele, C. A., Neidlinger-Wilke, C., Kaspar, D., Seidl, W., Margevicius, K. J., & Augat, P. (1998). Effects of mechanical factors on the fracture healing process. Clinical Orthopaedics and Related Research, 355(355 Suppl). https://doi.org/10.1097/00003086-199810001-00015

Claes, L., Augat, P., Suger, G., & Wilke, H. J. (1997). Influence of size and stability of the osteotomy gap on the success of fracture healing. Journal of Orthopaedic Research : Official Publication of the Orthopaedic Research Society, 15(4), 577–584. https://doi.org/10.1002/JOR.1100150414

Deitzel, J. M., Kleinmeyer, J., Harris, D., & Beck Tan, N. C. (2001). The effect of processing variables on the morphology of electrospun nanofibers and textiles. Polymer, 42(1), 261–272. https://doi.org/10.1016/S0032-3861(00)00250-0

Delhanty, P. J. D., van der Eerden, B. C. J., & van Leeuwen, J. P. T. M. (2014). Ghrelin and bone. BioFactors (Oxford, England), 40(1), 41–48. https://doi.org/10.1002/BIOF.1120

Denis, P., Dulnik, J., & Sajkiewicz, P. (2015). Electrospinning and Structure of Bicomponent Polycaprolactone/Gelatin Nanofibers Obtained Using Alternative Solvent System. International Journal of Polymeric Materials and Polymeric Biomaterials, 64(7), 354–364. https://doi.org/10.1080/00914037.2014.945208

Dhivya, S., Saravanan, S., Sastry, T. P., & Selvamurugan, N. (2015). Nanohydroxyapatite-reinforced chitosan composite hydrogel for bone tissue repair in vitro and in vivo. Journal of Nanobiotechnology, 13(1), 1–13. https://doi.org/10.1186/S12951-015-0099-Z/TABLES/2

Dimitriou, R., Jones, E., McGonagle, D., & Giannoudis, P. V. (2011). Bone regeneration: current concepts and future directions. BMC Medicine, 9, 66. https://doi.org/10.1186/1741-7015-9-66

Ding, D. C., Shyu, W. C., Lin, S. Z., & Li, H. (2007). The role of endothelial progenitor cells in ischemic cerebral and heart diseases. Cell Transplantation, 16(3), 273–284. https://doi.org/10.3727/000000007783464777

Dixon, D. T., & Gomillion, C. T. (2021). Conductive Scaffolds for Bone Tissue Engineering: Current State and Future Outlook. Journal of Functional Biomaterials 2022, Vol. 13, Page 1, 13(1), 1. https://doi.org/10.3390/JFB13010001

Dwivedi, R., Kumar, S., Pandey, R., Mahajan, A., Nandana, D., Katti, D. S., & Mehrotra, D. (2020). Polycaprolactone as a biomaterial for bone scaffolds: Review of literature. Journal of Oral Biology and Craniofacial Research, 10(1), 381. https://doi.org/10.1016/J.JOBCR.2019.10.003

Einhorn, T. A. (1996). Enhancement of fracture healing. Instructional Course Lectures, 45(6), 401–416. https://doi.org/10.2106/00004623-199506000-00016

Eltom, A., Zhong, G., & Muhammad, A. (2019a). Scaffold Techniques and Designs in Tissue Engineering Functions and Purposes: A Review. Advances in Materials Science and Engineering, 2019. https://doi.org/10.1155/2019/3429527

Eltom, A., Zhong, G., & Muhammad, A. (2019b). Scaffold Techniques and Designs in Tissue Engineering Functions and Purposes: A Review. Advances in Materials Science and Engineering, 2019. https://doi.org/10.1155/2019/3429527

Engelberg, I., & Kohn, J. (1991). Physico-mechanical properties of degradable polymers used in medical applications: a comparative study. Biomaterials, 12(3), 292–304. https://doi.org/10.1016/0142-9612(91)90037-B

Erener, T., Ceritoğlu, K. U., Aktekin, C. N., Dalgic, A. D., Keskin, D., Geneci, F., Ocak, M., Bilecenoğlu, B., Hücümenoğlu, S., Çaydere, M., Şeneş, M., & Sezgin, Ö. (2021). Investigation of the effect of ghrelin on bone fracture healing in rats. Clinical and Experimental Pharmacology & Physiology, 48(10), 1382–1390. https://doi.org/10.1111/1440-1681.13544

Ferrara, N. (2004). Vascular endothelial growth factor: basic science and clinical progress. Endocrine Reviews, 25(4), 581–611. https://doi.org/10.1210/ER.2003-0027

Ferrara, N., Gerber, H. P., & LeCouter, J. (2003). The biology of VEGF and its receptors. Nature Medicine 2003 9:6, 9(6), 669–676. https://doi.org/10.1038/nm0603-669

Filipowska, J., Tomaszewski, K. A., Niedźwiedzki, Ł., Walocha, J. A., & Niedźwiedzki, T. (2017). The role of vasculature in bone development, regeneration, and proper systemic functioning. Angiogenesis, 20(3), 291. https://doi.org/10.1007/S10456-017-9541-1

Flores-Rojas, G. G., Gómez-Lazaro, B., López-Saucedo, F., Vera-Graziano, R., Bucio, E., & Mendizábal, E. (2023). Electrospun Scaffolds for Tissue Engineering: A Review. Macromol 2023, Vol. 3, Pages 524-553, 3(3), 524–553. https://doi.org/10.3390/MACROMOL3030031

Forsythe, J. A., Jiang, B.-H., Iyer, N. V., Agani, F., Leung, S. W., Koos, R. D., & Semenza, G. L. (1996). Activation of vascular endothelial growth factor gene transcription by hypoxia-inducible factor 1. Molecular and Cellular Biology, 16(9), 4604–4613. https://doi.org/10.1128/MCB.16.9.4604

Fukushima, N., Hanada, R., Teranishi, H., Fukue, Y., Tachibana, T., Ishikawa, H., Takeda, S., Takeuchi, Y., Fukumoto, S., Kangawa, K., Nagata, K., & Kojima, M.

(2005). Ghrelin directly regulates bone formation. Journal of Bone and Mineral Research : The Official Journal of the American Society for Bone and Mineral Research, 20(5), 790–798. https://doi.org/10.1359/JBMR.041237

Gharibshahian, M., Salehi, M., Beheshtizadeh, N., Kamalabadi-Farahani, M., Atashi, A., Nourbakhsh, M. S., & Alizadeh, M. (2023). Recent advances in 3D-printed PCL-based composite scaffolds for bone tissue engineering. Frontiers in Bioengineering and Biotechnology, 11, 1168504. https://doi.org/10.3389/FBIOE.2023.1168504/BIBTEX

Glowacki, J. (1998). Angiogenesis in fracture repair. Clinical Orthopaedics and Related Research, 355(355 Suppl). https://doi.org/10.1097/00003086-199810001-00010

Haider, A., Haider, S., & Kang, I. K. (2018). A comprehensive review summarizing the effect of electrospinning parameters and potential applications of nanofibers in biomedical and biotechnology. Arabian Journal of Chemistry, 11(8), 1165–1188. https://doi.org/10.1016/J.ARABJC.2015.11.015

Haider, S., Al-Zeghayer, Y., Ahmed Ali, F. A., Haider, A., Mahmood, A., Al-Masry, W. A., Imran, M., & Aijaz, M. O. (2013). Highly aligned narrow-diameter chitosan electrospun nanofibers. Journal of Polymer Research, 20(4), 1–11. https://doi.org/10.1007/S10965-013-0105-9/FIGURES/3

Hausman, M. R., Schaffler, M. B., & Majeska, R. J. (2001). Prevention of fracture healing in rats by an inhibitor of angiogenesis. Bone, 29(6), 560–564. https://doi.org/10.1016/S8756-3282(01)00608-1

Hsieh, C. Y., Tsai, S. P., Wang, D. M., Chang, Y. N., & Hsieh, H. J. (2005). Preparation of γ-PGA/chitosan composite tissue engineering matrices. Biomaterials, 26(28), 5617–5623. https://doi.org/10.1016/J.BIOMATERIALS.2005.02.012

Huang, M.-N., Wang, Y.-L., Luo, Y.-F., Huang, M.-N., Wang, Y.-L., & Luo, Y.-F. (2009). Biodegradable and bioactive porous polyurethane scaffolds for bone tissue engineering. Journal of Biomedical Science and Engineering, 2(1), 36–40. https://doi.org/10.4236/JBISE.2009.21007

Islam, M. S., Ang, B. C., Andriyana, A., & Afifi, A. M. (2019). A review on fabrication of nanofibers via electrospinning and their applications. SN Applied Sciences, 1(10), 1–16. https://doi.org/10.1007/S42452-019-1288-4/TABLES/1

Jahed, E., Khaledabad, M. A., Almasi, H., & Hasanzadeh, R. (2017). Physicochemical properties of Carum copticum essential oil loaded chitosan films containing organic nano reinforcements. Carbohydrate Polymers, 164, 325–338. https://doi.org/10.1016/J.CARBPOL.2017.02.022

Janmohammadi, M., Nazemi, Z., Salehi, A. O. M., Seyfoori, A., John, J. V., Nourbakhsh, M. S., & Akbari, M. (2023). Cellulose-based composite scaffolds for bone tissue engineering and localized drug delivery. Bioactive Materials, 20, 137. https://doi.org/10.1016/J.BIOACTMAT.2022.05.018

Janmohammadi, M., Nazemi, Z., Salehi, A. O. M., Seyfoori, A., John, J. V., Nourbakhsh, M. S., & Akbari, M. (2023). Cellulose-based composite scaffolds for bone tissue engineering and localized drug delivery. Bioactive Materials, 20, 137–163. https://doi.org/10.1016/J.BIOACTMAT.2022.05.018

Jeong, J., Kim, J. H., Shim, J. H., Hwang, N. S., & Heo, C. Y. (2019). Bioactive calcium phosphate materials and applications in bone regeneration. Biomaterials Research, 23(1). https://doi.org/10.1186/S40824-018-0149-3

Jeong, S. I., Lee, A. Y., Lee, Y. M., & Shin, H. (2008). Electrospun gelatin/poly(L-lactide-co-ε-caprolactone) nanofibers for mechanically functional tissue-engineering scaffolds. Journal of Biomaterials Science, Polymer Edition, 19(3), 339–357. https://doi.org/10.1163/156856208783721029

Kim, S. W., Her, S. J., Park, S. J., Kim, D., Park, K. S., Lee, H. K., Han, B. H., Kim, M. S., Shin, C. S., & Kim, S. Y. (2005a). Ghrelin stimulates proliferation and differentiation and inhibits apoptosis in osteoblastic MC3T3-E1 cells. Bone, 37(3), 359–369. https://doi.org/10.1016/J.BONE.2005.04.020

Kim, S. W., Her, S. J., Park, S. J., Kim, D., Park, K. S., Lee, H. K., Han, B. H., Kim, M. S., Shin, C. S., & Kim, S. Y. (2005b). Ghrelin stimulates proliferation and differentiation and inhibits apoptosis in osteoblastic MC3T3-E1 cells. Bone, 37(3), 359–369. https://doi.org/10.1016/J.BONE.2005.04.020

Kneser, U., Schaefer, D. J., Munder, B., Klemt, C., Andree, C., & Stark, G. B. (2002). Tissue engineering of bone. Minimally Invasive Therapy and Allied Technologies, 11(3), 107–116. https://doi.org/10.1080/136457002320174177

Lalwani, G., D'Agati, M., Farshid, B., & Sitharaman, B. (2016). Carbon and inorganic nanomaterial-reinforced polymeric nanocomposites for bone tissue engineering. Nanocomposites for Musculoskeletal Tissue Regeneration, 31–66. https://doi.org/10.1016/B978-1-78242-452-9.00002-9

Liu, H., & Hsieh, Y. Lo. (2002). Ultrafine fibrous cellulose membranes from electrospinning of cellulose acetate. Journal of Polymer Science Part B: Polymer Physics, 40(18), 2119–2129. https://doi.org/10.1002/POLB.10261

Liu, H., Xu, G. W., Wang, Y. F., Zhao, H. S., Xiong, S., Wu, Y., Heng, B. C., An, C. R., Zhu, G. H., & Xie, D. H. (2015). Composite scaffolds of nano-hydroxyapatite and silk fibroin enhance mesenchymal stem cell-based bone regeneration via the interleukin 1 alpha autocrine/paracrine signaling loop. Biomaterials, 49, 103–112. https://doi.org/10.1016/J.BIOMATERIALS.2015.01.017

Long, Y. Z., Yan, X., Wang, X. X., Zhang, J., & Yu, M. (2019). Electrospinning: The Setup and Procedure. Electrospinning: Nanofabrication and Applications, 21–52. https://doi.org/10.1016/B978-0-323-51270-1.00002-9

Lukin, I., Erezuma, I., Maeso, L., Zarate, J., Desimone, M. F., Al-Tel, T. H., Dolatshahi-Pirouz, A., & Orive, G. (2022a). Progress in Gelatin as Biomaterial for Tissue Engineering. Pharmaceutics 2022, Vol. 14, Page 1177, 14(6), 1177. https://doi.org/10.3390/PHARMACEUTICS14061177

Lukin, I., Erezuma, I., Maeso, L., Zarate, J., Desimone, M. F., Al-Tel, T. H., Dolatshahi-Pirouz, A., & Orive, G. (2022b). Progress in Gelatin as Biomaterial for

Tissue Engineering. Pharmaceutics, 14(6). https://doi.org/10.3390/PHARMACEUTICS14061177

Maia, F. R., Bastos, A. R., Oliveira, J. M., Correlo, V. M., & Reis, R. L. (2022). Recent approaches towards bone tissue engineering. Bone, 154, 116256. https://doi.org/10.1016/J.BONE.2021.116256

Marsell, R., & Einhorn, T. A. (2011). The biology of fracture healing. J. Care Injured, 42, 551–555. https://doi.org/10.1016/j.injury.2011.03.031

Mathur, N., Mehdi, S. F., Anipindi, M., Aziz, M., Khan, S. A., Kondakindi, H., Lowell, B., Wang, P., & Roth, J. (2020). Ghrelin as an Anti-Sepsis Peptide: Review. Frontiers in Immunology, 11. https://doi.org/10.3389/FIMMU.2020.610363

McKeen, L. (2021). The Effect of Long Term Thermal Exposure on Plastics and Elastomers, Second Edition. The Effect of Long Term Thermal Exposure on Plastics and Elastomers, Second Edition, 1–336. https://doi.org/10.1016/C2020-0-02194-8

Mejía Suaza, M. L., Hurtado Henao, Y., & Moncada Acevedo, M. E. (2022). Wet Electrospinning and its Applications: A Review. TecnoLógicas, 25(54), e2223. https://doi.org/10.22430/22565337.2223

Mikos, A. G., Thorsen, A. J., Czerwonka, L. A., Bao, Y., Langer, R., Winslow, D. N., & Vacanti, J. P. (1994). Preparation and characterization of poly(l-lactic acid) foams. Polymer, 35(5), 1068–1077. https://doi.org/10.1016/0032-3861(94)90953-9

Mishra, R., & Kumar, A. (2011). Inorganic/organic biocomposite cryogels for regeneration of bony tissues. Journal of Biomaterials Science. Polymer Edition, 22(16), 2107–2126. https://doi.org/10.1163/092050610X534230

Nasr-Esfahani, M., & Mehrabanian, M. (2011). HA/nylon 6,6 porous scaffolds fabricated by salt-leaching/solvent casting technique: effect of nano-sized filler content on scaffold properties. International Journal of Nanomedicine, 1651. https://doi.org/10.2147/IJN.S21203

Nguyen, L. H., Annabi, N., Nikkhah, M., Bae, H., Binan, L., Park, S., Kang, Y., Yang, Y., & Khademhosseini, A. (2012). Vascularized bone tissue engineering: Approaches for potential improvement. Tissue Engineering - Part B: Reviews, 18(5), 363–382. https://doi.org/10.1089/TEN.TEB.2012.0012/ASSET/IMAGES/LARGE/FIGURE5.JPEG

Nosar, M. N., Salehi, M., Ghorbani, S., Beiranvand, S. P., Goodarzi, A., & Azami, M. (2016). Characterization of wet-electrospun cellulose acetate based 3-dimensional scaffolds for skin tissue engineering applications: influence of cellulose acetate concentration. Cellulose, 23(5), 3239–3248. https://doi.org/10.1007/S10570-016-1026-7/FIGURES/4

Ornitz, D. M., & Marie, P. J. (2019). Fibroblast growth factors in skeletal development. Current Topics in Developmental Biology, 133, 195–234. https://doi.org/10.1016/BS.CTDB.2018.11.020

Pant, B., Park, M., & Park, S. J. (2019). Drug Delivery Applications of Core-Sheath Nanofibers Prepared by Coaxial Electrospinning: A Review. Pharmaceutics 2019, Vol. 11, Page 305, 11(7), 305. https://doi.org/10.3390/PHARMACEUTICS11070305

Pillay, A., Sharma, K., & SubashiniM, M. (2013). Smart Tool for Integrated Chips Selection General Terms. International Journal of Computer Applications, 69(23), 975–8887.

Pina, S., Oliveira, J. M., & Reis, R. L. (2015). Natural-Based Nanocomposites for Bone Tissue Engineering and Regenerative Medicine: A Review. Advanced Materials, 27(7), 1143–1169. https://doi.org/10.1002/ADMA.201403354

Qu, H., Wei, S., & Guo, Z. (2013). Coaxial electrospun nanostructures and their applications. Journal of Materials Chemistry A, 1(38), 11513–11528. https://doi.org/10.1039/C3TA12390A

Rodríguez, K., Gatenholm, P., & Renneckar, S. (2012). Electrospinning cellulosic nanofibers for biomedical applications: Structure and in vitro biocompatibility. Cellulose, 19(5), 1583–1598. https://doi.org/10.1007/S10570-012-9734-0/TABLES/4

Roseti, L., Parisi, V., Petretta, M., Cavallo, C., Desando, G., Bartolotti, I., & Grigolo, B. (2017). Scaffolds for Bone Tissue Engineering: State of the art and new perspectives. Materials Science and Engineering: C, 78, 1246–1262. https://doi.org/10.1016/J.MSEC.2017.05.017

Seddiqi, H., Oliaei, E., Honarkar, H., Jin, J., Geonzon, L. C., Bacabac, R. G., & Klein-Nulend, J. (2021). Cellulose and its derivatives: towards biomedical applications. Cellulose 2021 28:4, 28(4), 1893–1931. https://doi.org/10.1007/S10570-020-03674-W

Semenza, G. L. (2000). HIF-1: mediator of physiological and pathophysiological responses to hypoxia. Journal of Applied Physiology (Bethesda, Md. : 1985), 88(4), 1474–1480. https://doi.org/10.1152/JAPPL.2000.88.4.1474

Semenza, G. L. (2003). Targeting HIF-1 for cancer therapy. Nature Reviews Cancer 2003 3:10, 3(10), 721–732. https://doi.org/10.1038/nrc1187

Semenza, G. L. (2010). HIF-1: upstream and downstream of cancer metabolism. Current Opinion in Genetics & Development, 20(1), 51–56. https://doi.org/10.1016/J.GDE.2009.10.009

Sharma, G. K., James, N. R., Sharma, G. K., & James, N. R. (2022). Electrospinning: The Technique and Applications. Recent Developments in Nanofibers Research. https://doi.org/10.5772/INTECHOPEN.105804

Sheen, J. R., Mabrouk, A., & Garla, V. V. (2023). Fracture Healing Overview. StatPearls. https://www.ncbi.nlm.nih.gov/books/NBK551678/

Sheikh, Z., Javaid, M. A., Hamdan, N., & Hashmi, R. (2015). Bone Regeneration Using Bone Morphogenetic Proteins and Various Biomaterial Carriers. Materials, 8(4), 1778. https://doi.org/10.3390/MA8041778

Shi, C., Yuan, Z., Han, F., Zhu, C., & Li, B. (2016). Polymeric biomaterials for bone regeneration. Annals of Joint, 1(9), 27–27. https://doi.org/10.21037/AOJ.2016.11.02

Shibuya, M., & Claesson-Welsh, L. (2006). Signal transduction by VEGF receptors in the regulation of angiogenesis and lymphangiogenesis. Experimental Cell Research, 312(5), 549–560. https://doi.org/10.1016/J.YEXCR.2005.11.012

Simunovic, F., & Finkenzeller, G. (2021). Vascularization Strategies in Bone Tissue Engineering. Cells, 10(7). https://doi.org/10.3390/CELLS10071749

Sinha, R. (2020). DEVELOPMENT OF CELLULOSE ACETATE-BASED SCAFFOLD FOR BONE TISSUE ENGINEERING APPLICATIONS.

Son, W. K., Youk, J. H., Lee, T. S., & Park, W. H. (2004). Electrospinning of ultrafine cellulose acetate fibers: Studies of a new solvent system and deacetylation of ultrafine cellulose acetate fibers. Journal of Polymer Science Part B: Polymer Physics, 42(1), 5–11. https://doi.org/10.1002/POLB.10668

Suamte, L., Tirkey, A., Barman, J., & Jayasekhar Babu, P. (2023). Various manufacturing methods and ideal properties of scaffolds for tissue engineering applications. Smart Materials in Manufacturing, 1, 100011. https://doi.org/10.1016/J.SMMF.2022.100011

Suamte, L., Tirkey, A., Barman, J., & Jayasekhar Babu, P. (2023). Various manufacturing methods and ideal properties of scaffolds for tissue engineering applications. Smart Materials in Manufacturing, 1, 100011. https://doi.org/10.1016/J.SMMF.2022.100011

Sung, H. J., Meredith, C., Johnson, C., & Galis, Z. S. (2004). The effect of scaffold degradation rate on three-dimensional cell growth and angiogenesis. Biomaterials, 25(26), 5735–5742. https://doi.org/10.1016/J.BIOMATERIALS.2004.01.066

Thavornyutikarn, B., Chantarapanich, N., Sitthiseripratip, K., Thouas, G. A., & Chen, Q. (2014). Bone tissue engineering scaffolding: computer-aided scaffolding techniques. Progress in Biomaterials, 3(2–4), 61–102. https://doi.org/10.1007/S40204-014-0026-7/TABLES/11

Thitiset, T., Damrongsakkul, S., Yodmuang, S., Leeanansaksiri, W., Apinun, J., & Honsawek, S. (2021). A novel gelatin/chitooligosaccharide/demineralized bone matrix composite scaffold and periosteum-derived mesenchymal stem cells for bone tissue engineering. Biomaterials Research, 25(1), 1–11. https://doi.org/10.1186/S40824-021-00220-Y/FIGURES/6

Tungprapa, S., Puangparn, T., Weerasombut, M., Jangchud, I., Fakum, P., Semongkhol, S., Meechaisue, C., & Supaphol, P. (2007). Electrospun cellulose acetate fibers: Effect of solvent system on morphology and fiber diameter. Cellulose, 14(6), 563–575. https://doi.org/10.1007/S10570-007-9113-4/TABLES/4

Van Leeuwen, A. C., Huddleston Slater, J. J. R., Gielkens, P. F. M., De Jong, J. R., Grijpma, D. W., & Bos, R. R. M. (2012). Guided bone regeneration in rat mandibular defects using resorbable poly(trimethylene carbonate) barrier membranes. Acta Biomaterialia, 8(4), 1422–1429. https://doi.org/10.1016/J.ACTBIO.2011.12.004

Visser, J., Gawlitta, D., Benders, K. E. M., Toma, S. M. H., Pouran, B., van Weeren, P. R., Dhert, W. J. A., & Malda, J. (2015). Endochondral bone formation in gelatin methacrylamide hydrogel with embedded cartilage-derived matrix particles. Biomaterials, 37, 174–182. https://doi.org/10.1016/J.BIOMATERIALS.2014.10.020

Wang, D. X., He, Y., Bi, L., Qu, Z. H., Zou, J. W., Pan, Z., Fan, J. J., Chen, L., Dong, X., Liu, X. N., Pei, G. X., & Ding, J. D. (2013). Enhancing the bioactivity of Poly(lactic-co-glycolic acid) scaffold with a nano-hydroxyapatite coating for the treatment of segmental bone defect in a rabbit model. International Journal of Nanomedicine, 8(1), 1855–1865. https://doi.org/10.2147/IJN.S43706

Wang, F., Tankus, E. B., Santarella, F., Rohr, N., Sharma, N., Märtin, S., Michalscheck, M., Maintz, M., Cao, S., & Thieringer, F. M. (2022). Fabrication and Characterization of PCL/HA Filament as a 3D Printing Material Using Thermal Extrusion Technology for Bone Tissue Engineering. Polymers, 14(4), 669. https://doi.org/10.3390/POLYM14040669/S1

Wang, L., & Stegemann, J. P. (2010). Thermogelling chitosan and collagen composite hydrogels initiated with β-glycerophosphate for bone tissue engineering. Biomaterials, 31(14), 3976–3985. https://doi.org/10.1016/J.BIOMATERIALS.2010.01.131

Wang, L., Chen, Q., Li, G., & Ke, D. (2012). Ghrelin stimulates angiogenesis via GHSR1a-dependent MEK/ERK and PI3K/Akt signal pathways in rat cardiac microvascular endothelial cells. Peptides, 33(1), 92–100. https://doi.org/10.1016/J.PEPTIDES.2011.11.001

Wang, W., & Yeung, K. W. K. (2017). Bone grafts and biomaterials substitutes for bone defect repair: A review. Bioactive Materials, 2(4), 224–247. https://doi.org/10.1016/J.BIOACTMAT.2017.05.007

Wang, X., Yang, L., Chen, Y., Zhang, L., & Fei, H. (2021). Ghrelin promotes angiogenesis by activating the Jagged1/Notch2/VEGF pathway in preeclampsia. The Journal of Obstetrics and Gynaecology Research, 47(2), 486–494. https://doi.org/10.1111/JOG.14555

Wei, S., Ma, J. X., Xu, L., Gu, X. S., & Ma, X. L. (2020). Biodegradable materials for bone defect repair. Military Medical Research 2020 7:1, 7(1), 1–25. https://doi.org/10.1186/S40779-020-00280-6

Yan, J., White, K., Yu, D. G., & Zhao, X. Y. (2014). Sustained-release multiple-component cellulose acetate nanofibers fabricated using a modified coaxial electrospinning process. Journal of Materials Science, 49(2), 538–547. https://doi.org/10.1007/S10853-013-7733-7/TABLES/2

Yang, J., Zhang, L., Ding, Q., Zhang, S., Sun, S., Liu, W., Liu, J., Han, X., & Ding, C. (2023). Flavonoid-Loaded Biomaterials in Bone Defect Repair. Molecules 2023, Vol. 28, Page 6888, 28(19), 6888. https://doi.org/10.3390/MOLECULES28196888

Yu, D. G., Li, X. Y., Wang, X., Chian, W., Liao, Y. Z., & Li, Y. (2013). Zero-order drug release cellulose acetate nanofibers prepared using coaxial electrospinning. Cellulose, 20(1), 379–389. https://doi.org/10.1007/S10570-012-9824-Z/FIGURES/7

Yue, S., He, H., Li, B., & Hou, T. (2020). Hydrogel as a Biomaterial for Bone Tissue Engineering: A Review. Nanomaterials, 10(8), 1–25. https://doi.org/10.3390/NANO10081511

Zhang, X., Zhang, Y., Ma, G., Yang, D., & Nie, J. (2015). The effect of the pre-frozen process on properties of a chitosan/hydroxyapatite/poly(methyl methacrylate) composite prepared by freeze-drying method used for bone tissue engineering. RSC Advances, 5(97), 79679–79686. https://doi.org/10.1039/C5RA14549J

Zhang, Y., Su, B., Venugopal, J., Ramakrishna, S., & Lim, C. (2007). Biomimetic and bioactive nanofibrous scaffolds from electrospun composite nanofibers. https://doi.org/10.2147/IJN.S2.4.623

Zhijiang, C., Yi, X., Haizheng, Y., Jia, J., & Liu, Y. (2016). Poly(hydroxybutyrate)/cellulose acetate blend nanofiber scaffolds: Preparation, characterization and cytocompatibility. Materials Science and Engineering: C, 58, 757–767. https://doi.org/10.1016/J.MSEC.2015.09.048

Zhou, J., Zhang, Z., Joseph, J., Zhang, X., Ferdows, B. E., Patel, D. N., Chen, W., Banfi, G., Molinaro, R., Cosco, D., Kong, N., Joshi, N., Farokhzad, O. C., Corbo, C., & Tao, W. (2021a). Biomaterials and nanomedicine for bone regeneration: Progress and future prospects. Exploration, 1(2). https://doi.org/10.1002/EXP.20210011

Zhou, J., Zhang, Z., Joseph, J., Zhang, X., Ferdows, B. E., Patel, D. N., Chen, W., Banfi, G., Molinaro, R., Cosco, D., Kong, N., Joshi, N., Farokhzad, O. C., Corbo, C., & Tao, W. (2021b). Biomaterials and nanomedicine for bone regeneration: Progress and future prospects. Exploration, 1(2). https://doi.org/10.1002/EXP.20210011

Ziello, J. E., Jovin, I. S., & Huang, Y. (2007). Hypoxia-Inducible Factor (HIF)-1 Regulatory Pathway and its Potential for Therapeutic Intervention in Malignancy and Ischemia. The Yale Journal of Biology and Medicine, 80(2), 51. /pmc/articles/PMC2140184/

APPENDICES

A. Calibration Curve

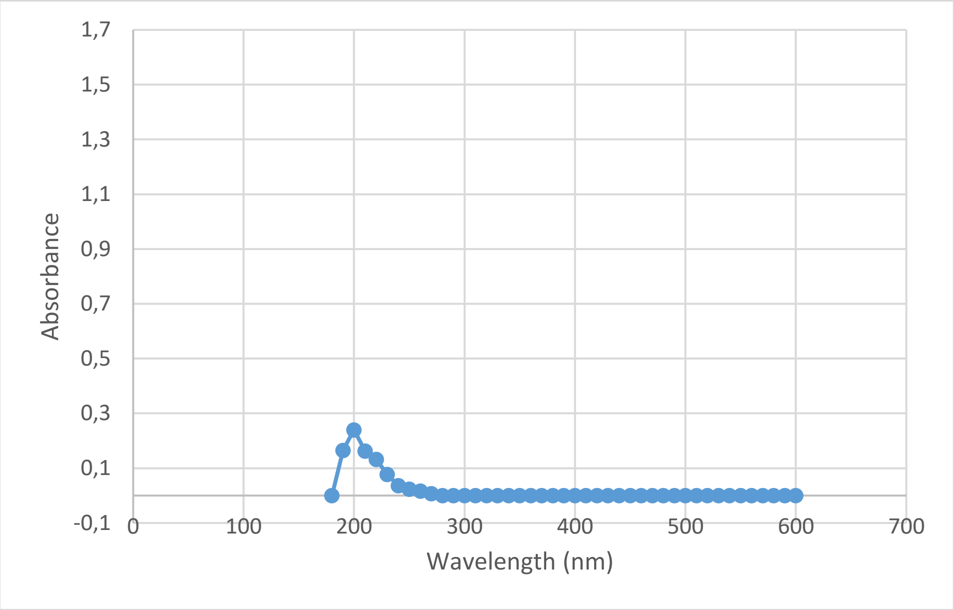

Figure 20. PBS wavelength scanning result.

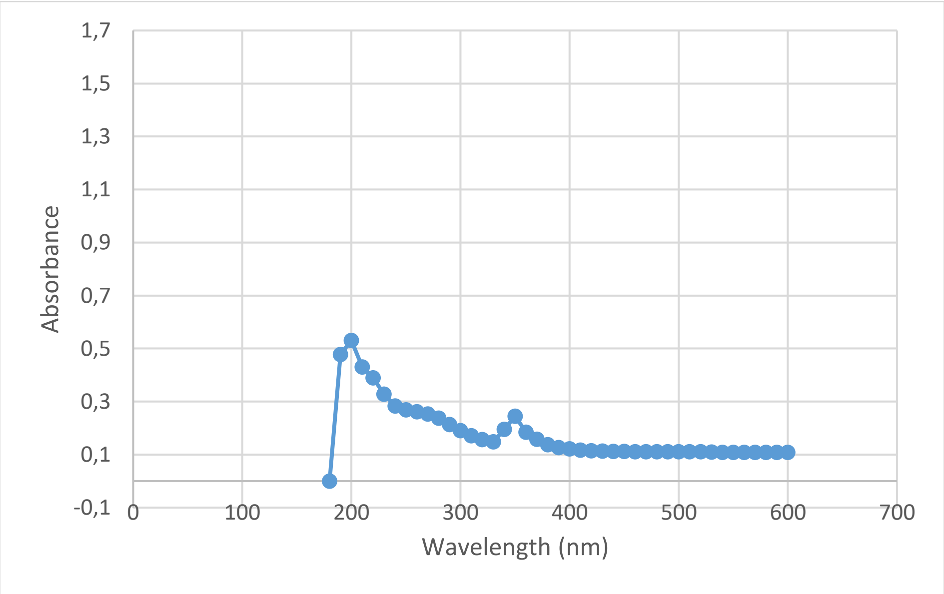

Figure 21. 100 nM ghrelin wavelength scanning result.

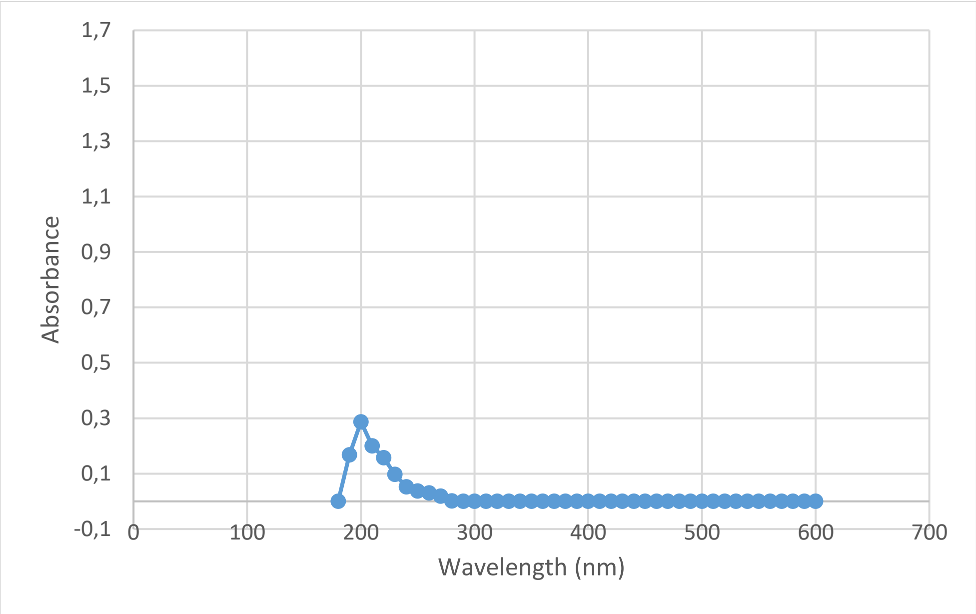

Figure 22. 8 ng/mL HIF1 α wavelength scanning result.

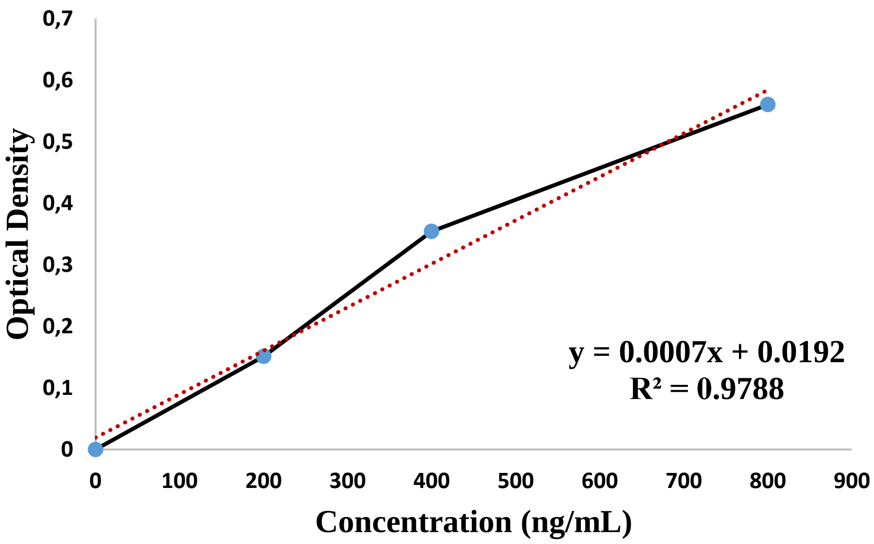

Figure 23. Calibration curve for VEGF using kit's standards at 450 nm (n=2).

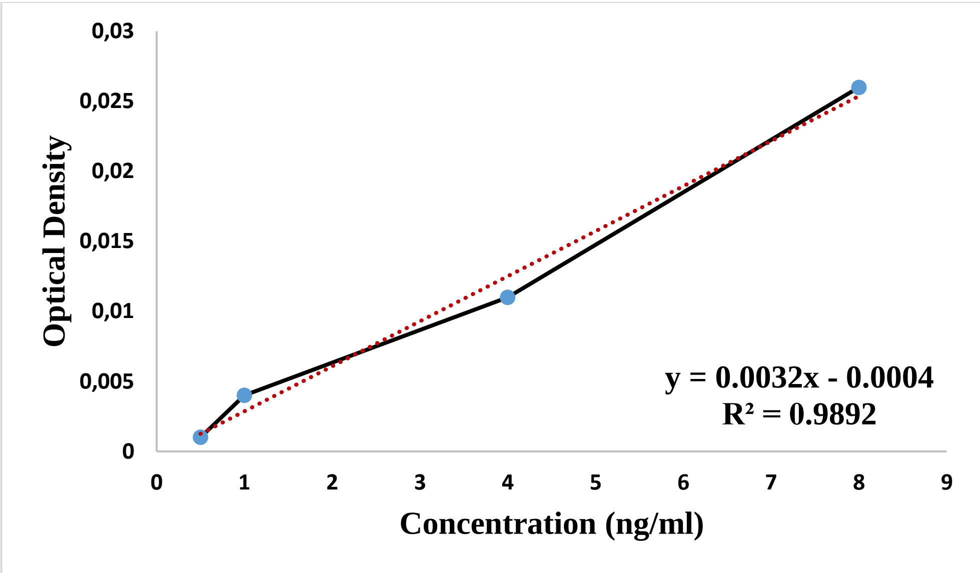

Figure 24. Calibration curve of HIF1 αconstructed with different concentrations of HIF1 alpha protein in PBS (7.4 pH) at 220 nm.

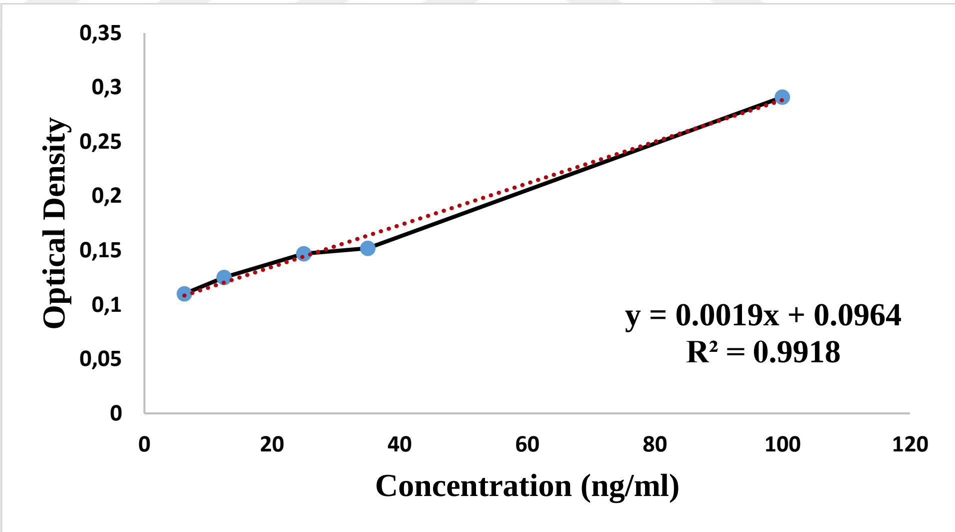

Figure 25. The calibration curve of Ghreline was constructed with different concentrations of Ghreline in PBS (7.4 pH) at 200 nm.

B. ALP Calibration Curve

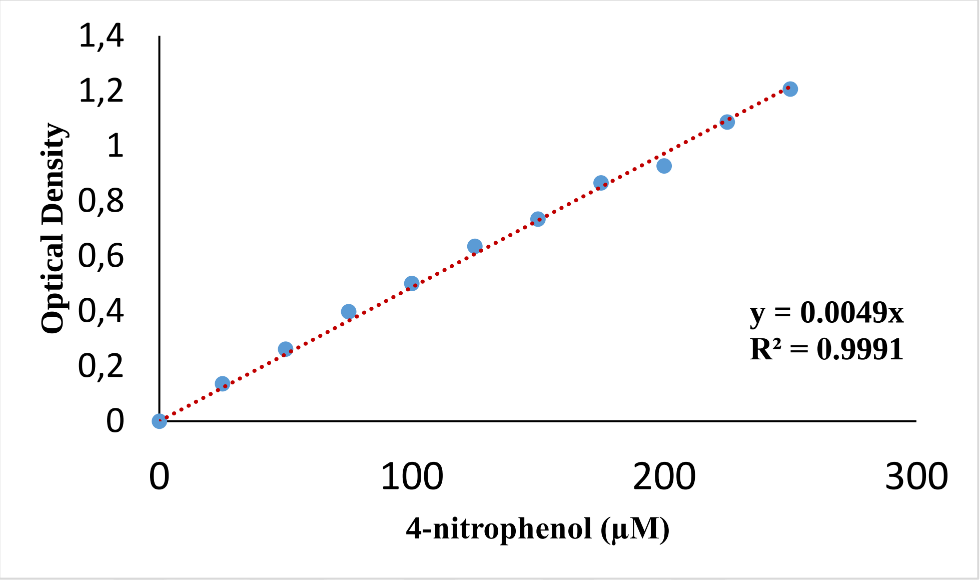

Figure 26. ALP calibration curve at 405 nm using various 4-nitrophenol concentrations in dH_2O (n=4).

C. Calcium Calibration Curve

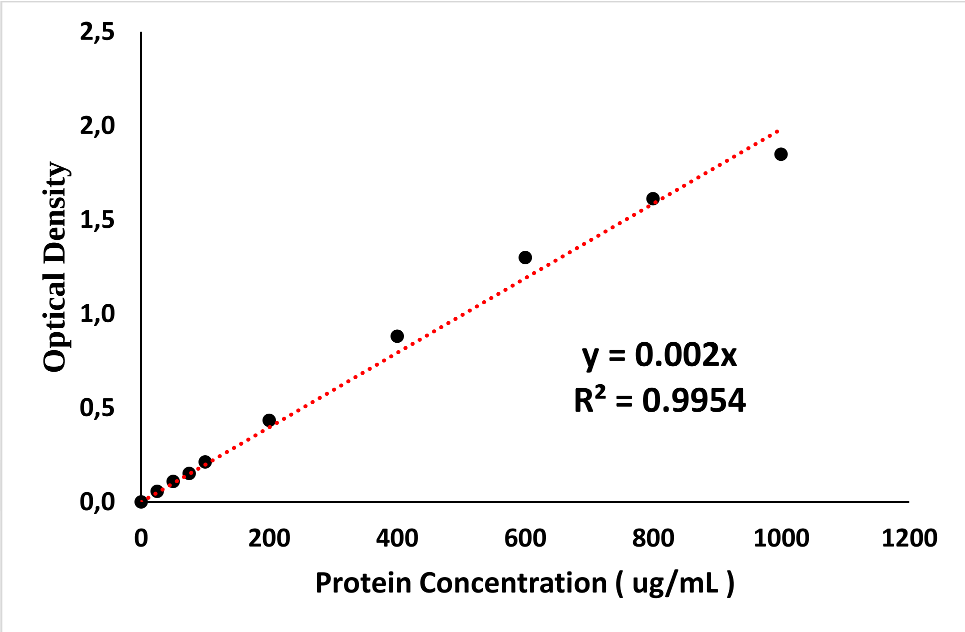

Figure 27. Calcium calibration curve using standard $CaCl_2$ values at 562 nm (n=5).